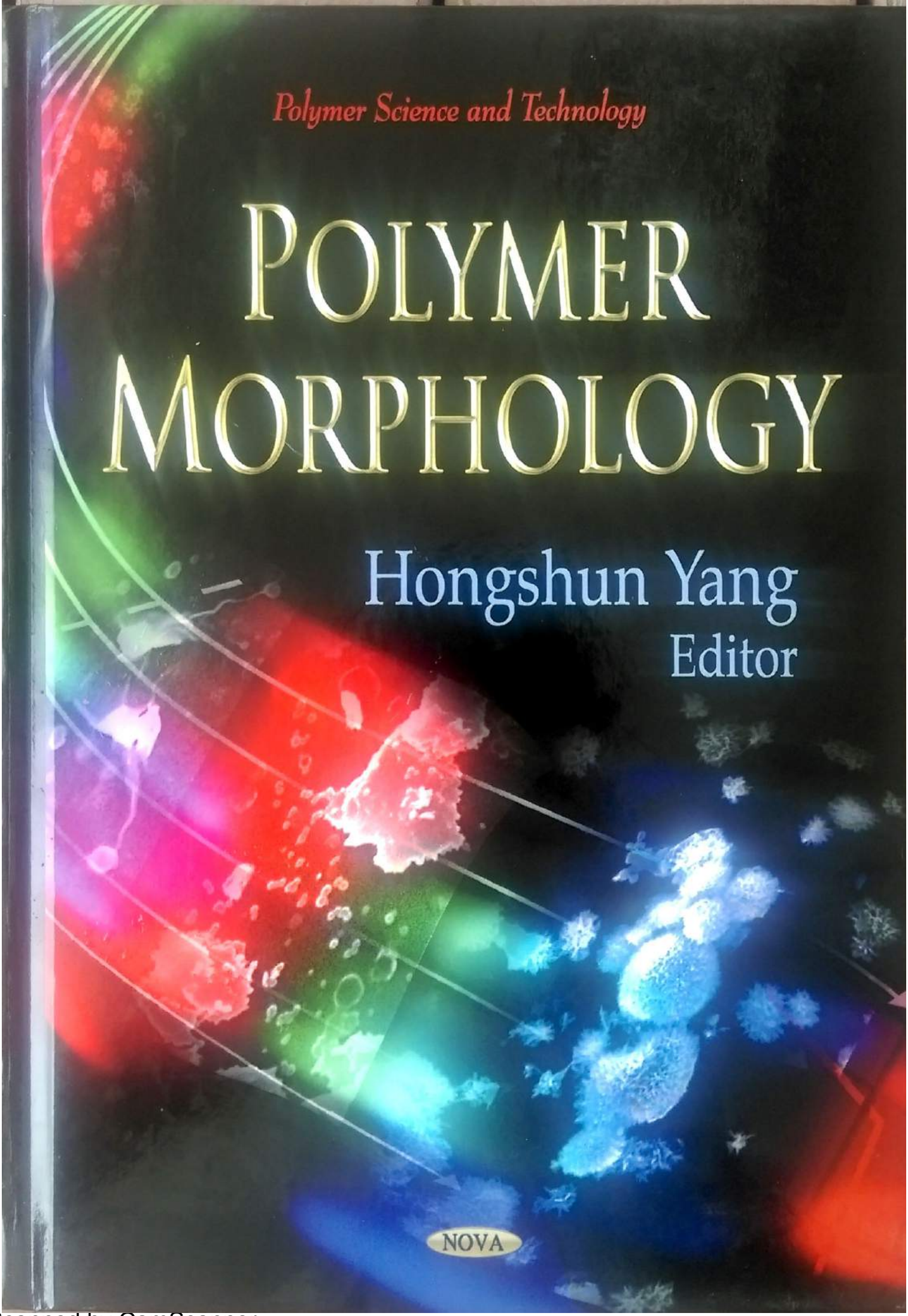

POLYMER SCIENCE AND TECHNOLOGY

POLYMER MORPHOLOGY

POLYMER SCIENCE AND TECHNOLOGY

POLYMER MORPHOLOGY

HONGSHUN YANG
EDITOR

Nova Science Publishers, Inc.
New York

CONTENTS

In: Polymer Morphology
Editor: Hongshun Yang

ISBN: 978-1-61470-880-3

Chapter 1

MORPHOLOGY ANALYSIS OF FRUIT POLYSACCHARIDES USING ATOMIC FORCE MICROSCOPY

Hongshun Yang[1,2,*], Hui Liu[3], Shaojuan Lai[4], and Fusheng Chen[1]

[1]College of Food Science and Technology, Henan University of Technology, 140 S Songshan Rd., Zhengzhou, Henan, China

[2]Department of Food Science and Nutrition, University of Minnesota, St. Paul, MN, US

[3]Zhengzhou Fruit Research Institute, Chinese Academy of Agricultural Sciences, Zhengzhou, Henan, China

[4]Department of Biochemistry, Molecular Biology and Biophysics, University of Minnesota, Minneapolis, MN, US

ABSTRACT

Fruit polysaccharides are major contributors for maintaining the texture of fruits and vegetables. The changes of fruit carbohydrates affect fruit quality and marketing value. While traditional physiochemical characterization and instrumental analysis of fruit polysaccharides could provide general structural information about fruit polysaccharides, they could not characterize the highly heterogeneous structures. Atomic force microscopy (AFM), which utilizes the molecular interaction between tip and sample, is a powerful tool for investigating the morphology of fruit polysaccharides at nano scale. In this review, the fundamentals of AFM including principle, sample preparation, on-line imaging and manipulation, and off-line result analysis were reviewed. Applications of AFM in fruit polysaccharides, including qualitative and quantitative analysis, as well as characterization and manipulation of fruit polysaccharides with AFM were introduced. The relationship of polysaccharide morphology with physiochemical analysis obtained from other techniques was also illustrated. The results indicate that AFM of fruit polysaccharides could reveal in-depth knowledge on fruit properties. Morphology of fruit polysaccharides investigated by AFM had good correlation with physicochemical properties determined by other techniques. The AFM results of fruit polysaccharides

* Corresponding author. Tel: +86-371-67789991; fax: +86-371-67756856. E-mail address: hongshunyang@hotmail.com (H. Yang).

could be used to elucidate the mechanism of quality changes of fruits during storage and processing.

Keywords: Atomic force microscopy (AFM); Fruits; Polysaccharides; Nanostructure; Quality

1. FUNDAMENTAL OF AFM

1.1. Introduction

Microscopy methodology has advantages over many other characterization techniques in that it can directly visualize the heterogeneity of samples. However, at molecular or nanoscale level, some microscopies can not provide images of enough resolution when images' sizes are small. Microscopic analysis at the single molecule level can be achieved by scanning probe methods including atomic force microscopy (AFM). AFM was developed in order to overcome a basic drawback of scanning tunnel microscopy (STM)-that it can only image conducting or semiconducting surfaces. AFM does not have this drawback, being able to image almost any type of surface, including polymers, ceramics, composites, glasses, and biological samples. It requires neither a vacuum environment nor any special sample preparation. In addition, it can be used in either an ambient or liquid environment [1].

AFM, as a nanotechnology instrument, is powerful in investigating food and biological materials [2]. It can provide high magnification three-dimensional images with high resolution, and measure samples with an analysis software without sophisticated preparation of the samples, allowing users to directly observe the samples under near their native status [3].

AFM also has other advantages over conventional microscopy techniques. It is one of the most advanced tools for imaging, measuring, and manipulating materials or objects at nanoscale with very high-resolution. The image resolution of AFM can be achieved on the order of fractions of one nanometer or less, more than 1000 times higher than the optical diffraction limit. Information of the materials or objects scanned is collected by "feeling" the surface with a mechanical probe. Piezoelectric elements that control the tiny but accurate and precise movements with the control of software enable a precise scanning.

1.2. Principle of AFM

AFM probes samples and makes measurements in three dimensions, x, y, and z (normal to the sample surface), thus enabling a presentation of three-dimensional images of a sample surface by measuring forces between a sharp probe (<10nm) and surface at very short distance (0.2-10 nm probe-sample separation) [4]. AFM images are obtained through determining the changes in the magnitude of interactions between AFM probe and the surface of samples when the surface is scanned by the probe. The interactions are commonly due to the van der Waal's force [5].

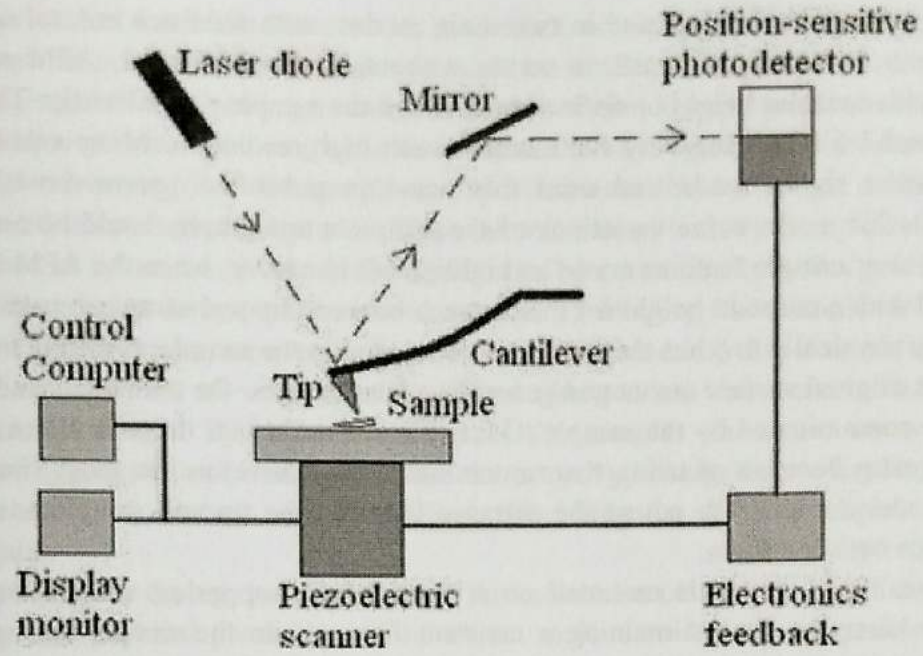

Figure 1. Schematic image of the AFM imaging process. Reprinted with permission from Journal of Food Science 2007, 72, R65-75. Copyright (2007), John Wiley and Sons, Inc [5].

Figure 1 shows the operation of an AFM system. A flexible cantilever with a sharp tip at one end scans in the x, y plane directions over the sample surface. A laser beam is focused on the back of the cantilever and reflected toward a quadrant photodiode detector by a mirror. During scanning, as the tip moves in response to different sample topographies, the angle of the reflected laser beam changes according to Hooke's law ($F = -kx$ where F is force, k is the spring constant, and x is the cantilever deflection). The minute changes in the deflection of the cantilever in the z axis caused by varying interaction forces between the apex of the tip and the sample surface are detected by a photodiode detector. Current signals from the segmented photodiode detector are utilized as a sensitive measure of the forces generated during the scanning by the AFM probe, and these current signals can be used as data for describing or reflecting topographies or other surface properties (visco-elasticity, for instance).

The difference in laser intensity between the segments of the quadrant photodiode detector generates an electrical signal which quantifies the movement of the AFM tip (for feedback loop, tip–sample separation maintains constant through moving the scanner in z direction for maintaining the set point deflection). Through maintaining a constant tip-sample separation and using Hooke's Law, the force between the tip and sample can be quantitatively calculated. Then, the distance that the scanner moves in the z direction is recorded by a computer, which is combined with the spatial variation in the x-y plane to generate the whole topographic image of the sample surface. When the sample is scanned by the AFM tip, the variation of the topography of the sample surface makes the cantilever deflection as the force (interaction) between the tip and sample changes. The image of the surface topography from the measured cantilever deflection can be generated by a computer and shown in a monitor, while the window of control software can be shown in another monitor. The topography information reflects the height of the sample directly, obtained by recording the changes in the z movement of the piezoelectric scanner that is needed to maintain the cantilever deflection constant with constant force mode [5, 6].

AFM scanning can be operated in two main modes: with feedback control and without feedback control. When the mode is set to without feedback control, AFM scanning is conducted with constant height or deflection between the sample and AFM tip. This mode is especially useful for imaging very flat samples with high resolution. Many scholars named this mode error signal mode and used this name in published peer-reviewed scientific literatures. In this mode, some variations of the sample's topography could be removed and the boundaries of sample features could be highlighted. However, when the AFM experiment is conducted with a constant height for the distance between tip and sample, one disadvantage is that the tip physically touches the surface or is trapped in the sample, resulting in damaging the sample's original surface status and generating false images. On the other hand, the AFM tip could be contaminated by the sample. Once it is contaminated, it could affect the images of next scanning because of using the contaminated tip. Therefore, in most situations, the feedback mode is applied to adjust the distance between the tip and sample to maintain a constant force between them.

Traditionally, a sample is mounted on a piezoelectric supporter, which can move the sample in z direction for maintaining a constant force while the sample is scanned with changing x and y directions. Otherwise, an alternative configuration of three piezo crystals can be utilized, with each crystal responsible for the changes in x,y and z directions, respectively. Thus a topographical or height mode image will be generated. In this situation, the distortion effects are minimized because of the scanner. In some newer models, AFM tip is mounted on a vertical piezo scanner while the sample is being scanned in X and Y with another piezo block.

Table 1 shows a comparison between AFM and other microscopes with regard to their advantages and disadvantages.

Table 1. Advantages and disadvantages of different microscopy techniques

Characteristics	Microscopy				
	AFM	LM	SEM	TEM	CLSM
Advantages	High resolution, nanoscale Minimal sample preparation, near native status 2D and 3D In air/liquid, in situ, continuous process Can be manipulated	Large scan area Fast scan speed Cheap	Nanoscale High resolution Fast scan speed	Nanoscale High resolution Fast scan speed	Study dynamic process Fast scan speed 2D and 3D In situ
Disadvantages	Small scan size Slower scan speed Difficult for soft material	Only 2D Need pretreatment Low resolution and magnification	Only 2D Need pretreatment Not native status	Only 2D Need pretreatment Not native status	Complicated operation Need pretreatment

Reprinted with permission from Journal of Food Science 2007, 72, R65-75. Copyright (2007), John Wiley and Sons, Inc [5].

1.3. Sample Preparation

Currently, most of the AFM systems are designed to be very use friendly and ideal for the beginners for doing their research. Samples can be imaged in air or fluid according to user's demands. Once the sample state (liquid or solid) and purpose of the scanning are determined, users can determine the imaging mode for their imaging. It should be noted that different companies might use different names for their individual modes, for instance, Digital

Instruments Co., Ltd named its three modes as contact, non-contact, and tapping for imaging, although these names of different companies might be similar.

For imaging a sample in air, generally a sample solution at appropriate concentration can be vortexed by a vortexer for being even distributed, then a drop of liquid solution (generally dozens of μl are enough) of the sample is deposited onto the surface of a flat supporter, freshly cleaved mica sheet, for instance. Then the mica sheet with the sample solution is put in a glove box at a low relative-humidity which can be controlled by silica gel. Some AFM equipment also has a temperature control system. If imaging the sample demands high requirements for cleanness, samples with mica can be air-dried in a dust-free enclosure which can be achieved by free air convection or forced nitrogen gas convection. Then the dried samples can be imaged by AFM scanning. If the samples show too many individual molecules or aggregates to clearly determine the property of targeted molecules, we can go back to the steps of diluting sample solution, depositing the diluted sample, drying, and imaging again.

During sample's drying, manipulation of the molecules could help better determine the morphology and physical properties of the object molecules. Take pectin molecules as an example, aggregation of pectin molecules or entanglement of pectin linear molecules would make individual observable molecular features un-differential. Manipulation of sample solutions after being deposited onto the mica surface could extend the pectin chains and make it possible for us to determine the length of pectin molecules accurately. Molecular combing and fluid fixation are two commonly used techniques to manipulate the molecules.

While fluid fixation utilizes velocity gradient of the convective fluid flow generated by evaporation of the droplet, molecular combing can be achieved by operating with a glass cover slip to comb the solutions and a reasonable pressure with a finger (fingers) on the glass cover slip while combing. Either one of the two treatments can yield well-elongated and aligned macromolecules, pectins, for instance. With the help of manipulation, AFM imaging can be used to investigate more delicate and detailed structural information [7].

Another commonly used method for extending sample chains is heating after dropping the sample. It was found that the presence of protein attached to polysaccharide might account for the need of substrate heating in order to allow the pectin to spread on the mica sheet surface [8]. When the sample was dropped onto a mica surface, the protein of the sample would be concentrated at the air-water interface as the solvent evaporates, thus the protein would aggregate. This aggregation process could be prevented by heating the substrate. Heating would evaporate the solvent more uniformly and rapidly to aid spreading the pectin molecules on the substrate.

It should be noted that manipulation processing might affect the targeted parameters determined by AFM. One example is that the height of liposomes measured from AFM was less than geometric mean diameter due to lipid spreading or flattening of liposomes during sample preparation [9]. This drawback has aroused researchers' concerns and they are developing some effective sample preparation methods to prevent the problem.

1.4. On-Line Imaging and Manipulation of AFM

A laboratory set up of an AFM includes a scanner, a sample and image display screen, a control screen, and a processor. A special table to isolate mechanical and acoustical vibrations

is highly recommended for performing high quality imaging. During scanning and data analysis, AFM software is used in a process that is divided into two stages: real-time operation and off-line analysis.

The purpose of real-time operation is to obtain images while the purpose of off-line analysis is to analyze the results (images) from real-time operation. The AFM can be real-time operated in several modes with other controlling signals or derivative data including phase shift and amplitude. During operation, imaging conditions can be controlled or modified through a computer. The changing conditions will generate corresponding electronic signals transmitted to the computer. The generated data can then be stored for further analysis in the off-line mode of AFM operation [5].

The function of real time operation is to run an actual microscope, change the size and location of the sample being scanned, control gains, etc. Scanner settings, such as scan area, vertical range and scan rate can be set according to the object properties [5]. Though the process of scanning is straightforward, not all images obtained accurately represent the actual topography information of a sample.

During scanning, there are parameters including control gains, which can be changed in each scan. The force used for imaging can also be altered for imaging each sample. Other commonly used parameters in real-time operation are setpoint and integral gain. During scanning, for getting more details on a special feature of a sample, the scanner can be adjusted to select and capture a small area within the region scanned.

Recently, force spectroscopy has become one of the hottest issues in imaging mode. In this mode, a macromolecule sample (pectin solution, for instance) is deposited onto a solid substrate (freshly mica sheet, for instance), then the AFM tip is brought into contact with the substrate through moving the piezotube. The chains of the macromolecule can absorb onto the AFM tip forming a structure like bridge between the tip and the substrate. Then this chain bridge will be stretched once the tip and the substrate separates, which causes the deflection of the cantilever. At the same time, deflection of the cantilever and displacement of the piezotube are recorded by a controlling computer. The deflection is then converted into force signals and the relationship between the force and the extension will be obtained. Thus, this imaging mode made a great performance on individual molecules and colloidal interactions [5, 10, 11].

Generally speaking, tapping mode AFM is the most suitable for most of food and biological samples because these samples are relatively soft. However, to choose an appropriate operation mode, one important thing is to optimize the method used. Users should always modify the procedure from published articles according to the specific properties of their samples including aggregation and elasticity, and accordingly choose appropriate tips and imaging conditions.

1.5. Off-Line Result Analysis

During AFM image's recording, a large amount of data are processed in real-time. There are mainly three tasks that should be conducted during real-time processing: conversion of analog signal to digital signal, transfer of data into computer memory and data displaying and/or saving [12].

For analyzing on-line data, images produced from on-line scans can be analyzed and/or modified using the software's offline functions. Almost each company has its own AFM software for analyzing AFM images. However, most of the functions of these softwares are similar and the results from different AFMs are comparable.

There are many offline operations that can be used for obtaining specific properties of the sample imaged. For example, sectional profile analysis can be used to measure dimensional properties like depth, height, and width of samples. Roughness analysis can be performed over any part selected of the image or the entire image to indicate the surface status of the samples.

Many modification functions of off-line software can be used to improve the quality of the image obtained from on-line scan. This improvement by off-line analysis software can reduce the noise caused during scanning and help obtain high quality images. One example is filters that can be used for improving the quality of AFM images. Another example is flattening which can be applied for removing artifacts of images due to vertical scanner drifts, image bows, skips, or others that might have resulted in a vertical offset between scan lines. However, any modification operation might affect the measurement of target objects, thus it is recommended to modify the images as little as possible if the quality of the images does not affect the calculation of the final results. Before any modifications, we need to realize the possible influences of that operation on the parameters we want to determine. An operation can not be performed if it would change the targeted parameters. For instance, if we want to get the roughness of a targeted sample or specific area, it is recommended not to use the flatten operation for the images, while flattening operation almost does not influence the dimensions of macromolecule chains, chain width of pectin, for instance [5].

In addition to the parameters provided by the software, properties of molecule studied can be utilized to acquire desired information. An example is measuring the heights of molecular chains to judge whether molecular intersections are branched places within molecules or overlapping among molecules. A perpendicular line can be drawn across the molecular chains studied, thus a vertical profile along that line will be displayed on the computer screen. A few couples of cursors can be placed along the line section for vertical measuring, and the results are viewed as the heights of molecular chains. A simple judgment is that the height of the chains is roughly equal to the sum of two single chains if two chains are overlapped while equal to the height of a single chain at branch points within the molecule [13]. The bright and dark areas in the images correspond to peaks and troughs in the objects, respectively. Commonly, different scales are used in the vertical and horizontal axes, respectively.

Recently, phase imaging and force spectroscopy have been developed and utilized for investigating more information on the mechanical properties of samples. Force spectroscopy utilizes the measurement of force-distance curve, which is based on the status including two quantities, cantilever deflection and polymer extension length. The cantilever is oscillated at its resonant frequency during the force-distance curve movement. During all the measurements, since many parameters including frequency, amplitude, phase of the excitation signal and the speed of z-piezo scanner movement are maintained constant, variations in mechanical properties-related outputs including composition, friction, chain stiffness, and viscoelasticity can be calculated from these curves [5, 14].

2. Application of AFM In Characterization of Fruits

2.1. Fruit Cell Wall

AFM can be applied to characterize the morphology of whole fruit surface, cell wall materials extracted, fruit polysaccharides including pectin, hemicellulose and cellulose. For characterizing cell wall materials or fruit polysaccharides, these components need to be extracted and purified first.

An example of extraction of cell wall materials, different pectins and hemicellulose from Chinese cherry was described [15]. About 10 g cherry flesh was rapidly pestled in an ice-cold mortar, then transferred into boiling ethanol for 20 min. After filtration, the residue was extracted again with ethanol for two more times. All the above extraction steps were repeated three times and supernatants collected together. Then the residue was incubated with dimethylsulphoxide (DMSO):water (9:1 as volume ratio) for removing starch, washed by water and transferred to chloroform:ethanol (2:1). The sample was filtrated and washed with 200 mL acetone until totally whitening, and then the cell wall material was obtained. For extracting pectins and hemicellulose, cell wall material was dissolved in sodium acetate buffer. After centrifugation, the water-soluble component was collected as water-soluble pectin. The water-insoluble pellet was transferred to sodium acetate buffer containing trans-1,2-diaminocyclohexane-N,N,N',N'-tetraacetic acid (CDTA), the soluble component was collected as chelate-soluble pectin (CSP). Residue was then resuspended in Na_2CO_3/CDTA, shaken and centrifuged. Soluble component was collected and named sodium carbonate-soluble pectin (SSP). The final extraction was performed using NaOH/$NaBH_4$. The solution was centrifuged and the extraction was repeated twice. Filtrates from the three consecutive extractions were pooled and referred to as hemicellulose fraction (HC). Further extraction of the insoluble part could yield the component of cellulose.

Cell wall materials can be imaged by AFM with a simple preparation step. Figure 2 shows AFM images of Chinese water chestnut cell walls. These images were shown with different modes for strengthening different morphology characteristics. Figure 2a shows a topographical image with the bright and dark areas in the image corresponding to peaks and troughs of the cell wall surface. Fibrous structures can be seen in brighter regions of the image. Figure 2b shows an error signal mode image. This mode imaging flattens the rough surface effectively and generates a better visual impression of the structure within the surface (Figure 2b). Cell wall materials are shown as laminated fibrous structures. But it should be noted that it is impossible to measure the layer thickness or fiber diameter accurately from the error signal mode image. For topographical image, the number of grey levels needed to indicate an image is too large to be discriminated by naked eyes. Therefore, regions of the troughs in the image appear devoid of structures. To solve this problem, it is necessary to isolate the structural information between the high frequency and low frequency of the cell wall surface. High pass filtering, and point smoothing and subtraction are two generally used methods to attain this purpose. High pass frequency filtering improves the image by setting threshold frequency (Figure 2c). Point smoothing and subtraction is used to locally average or smooth the image, which can eliminate molecular information and generate image of the curved surface. Then uneven surface can be subtracted from the topographical image and generate 'flattened' projection of the surface (Figure 2d).

Figure 3 shows representative images of the parenchyma cell wall surface chosen from over 500 AFM images taken from different maize parenchyma. Parenchyma cells from maize have a typical polyhedral-shaped wall and are 150-200 μm in diameter. In light microscopy (Figure 3A), the thin nonlignified cell walls were relatively transparent and featured primary pits [17]. Generally, the primary walls appear rather "clean" with sheets of fibers apparent (Figure 3B and H) [17]. These structures are hundreds of nanometers in size (Figure 3E). Occasional cell wall depressions (Figure 3C) and rugae were also observed. Insertion of particle-like materials between the lamellae could also have the ridge effect (Figure 3I). There were two different types of cell wall depressions: primary pits (Figure 3C) and primary pit-fields (Figure 3D) [17]. The microfibrils showed different appearances, from clearly defined (Figure 3H) to fully embedded in the cell wall matrixes (Figure 3I and J). These structures seemed to be found only on the uppermost surface of some parenchyma cell walls (Figure 3F and G) but not found in the cell walls where the microfibrils appeared to be heavily coated with possible hemicelluloses/pectin matrixes (Figure 3I and J).

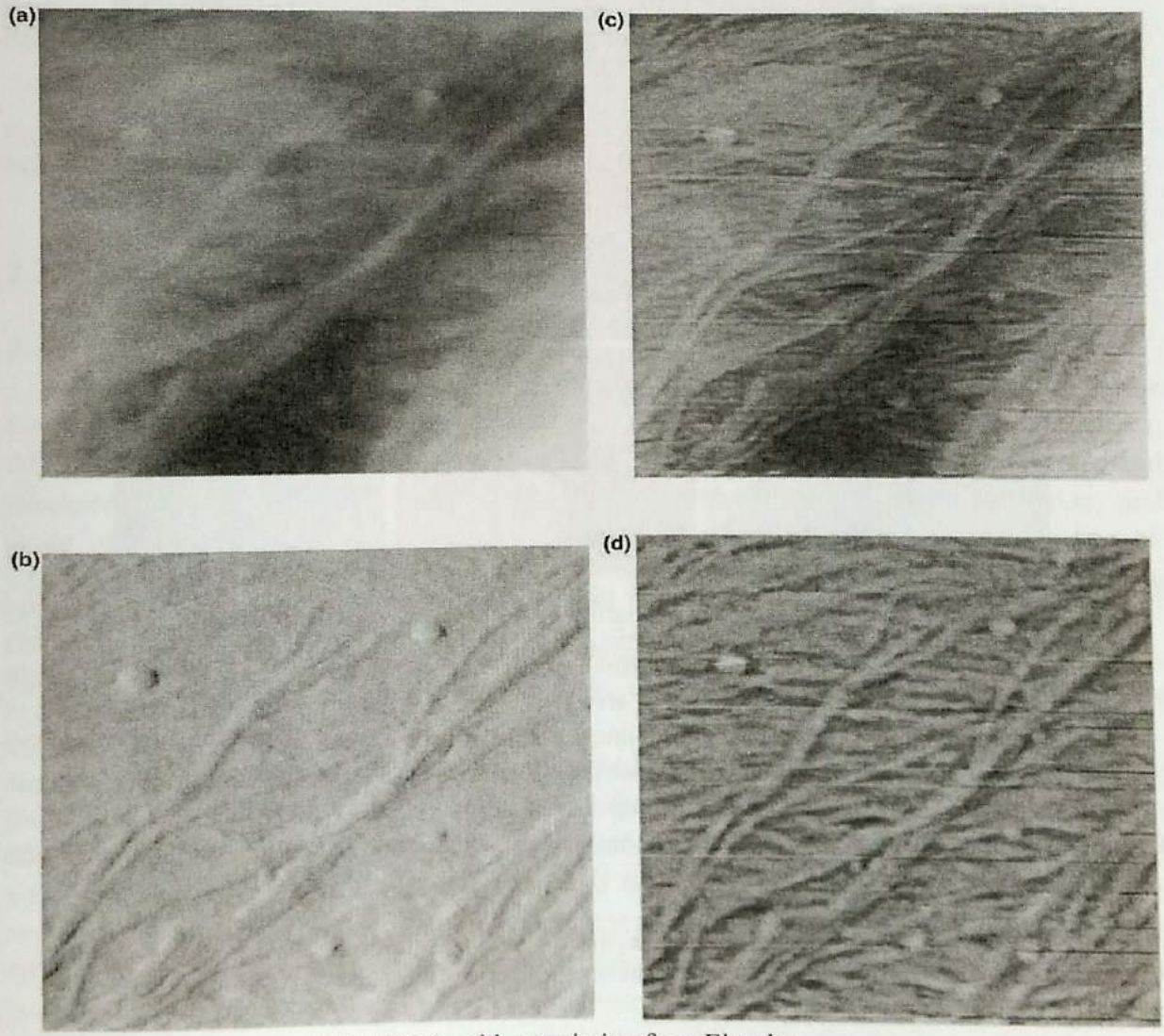

Reprinted from [16], Copyright (1997), with permission from Elsevier.

Figure 2. AFM images of Chinese water chestnut cell walls. (a) DC contact constant force image. (b) Complimentary error signal mode image. (c) Effect of high pass filtering. (d) Effect of point smoothing and subtraction. All scan sizes are 0.5 μm × 0.5 μm.

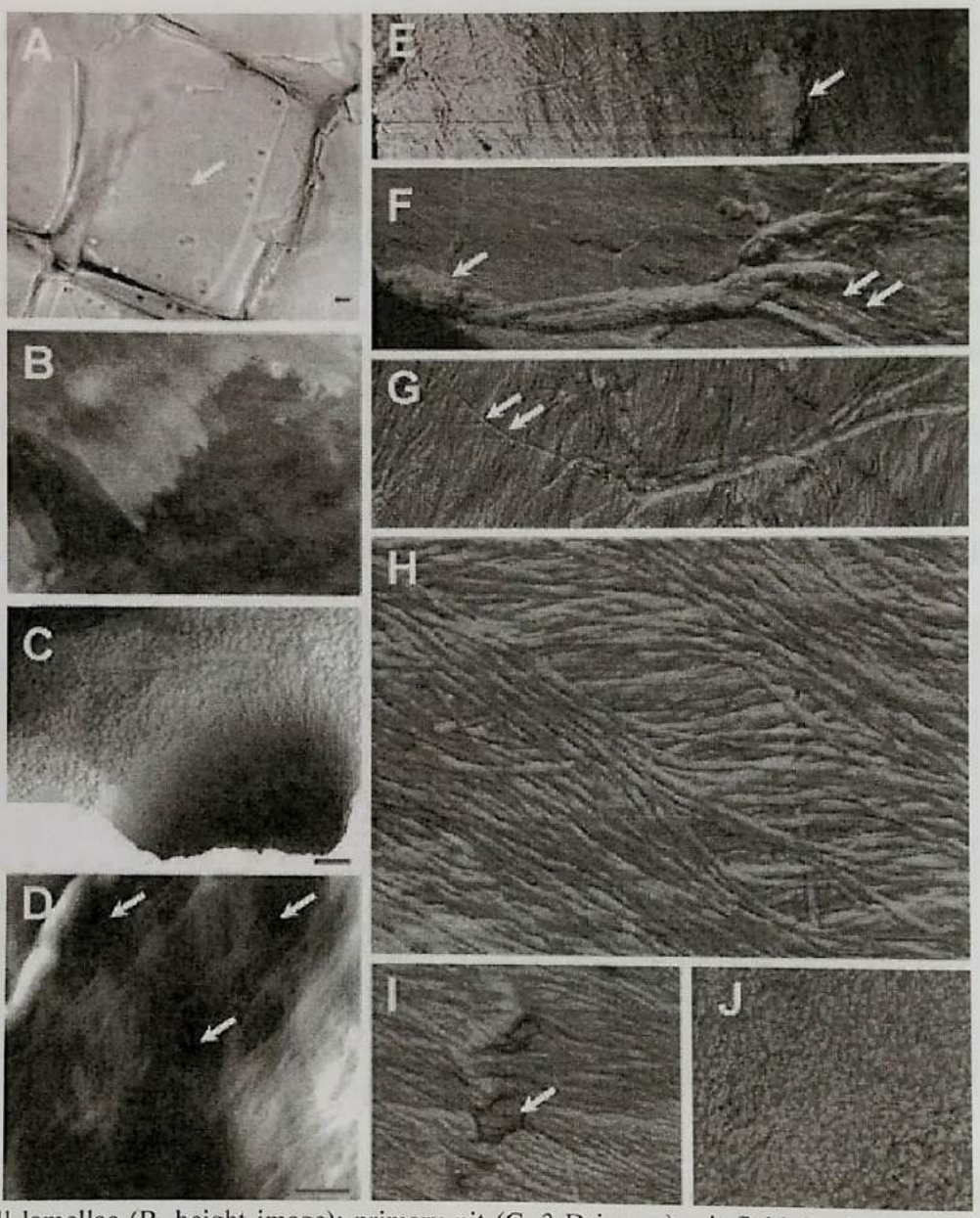

Note: wall lamellae (B, height image); primary pit (C, 3-D image); pit-field (D, height image); dried cytoplasm remnants or membrane debris (E, phase image); a process of synthesis of elementary fibrils-macrofibrils-micrifibrils (white arrow), phase image; a number of elementary fibrils coalesce into a macrofibril (double white arrow) (G, phase image); newly synthesized sheets of parallel-oriented microfibrils (H, phase image); microfibrils coated with more non-cellulosic polymers, and particles embedded in the matrixes (I, phase image); and more cell wall components deposited in the wall matrixes (J, phase image).

Figure 3. Primary cell walls from maize parenchyma. (A) A light microscopy image shows a fairly transparent primary wall with primary pits (white arrow), scale: 10 μm. (B-J) AFM mapping of wall surfaces, scale: 200 nm.

Figure 4 presents a high-resolution AFM height image showing a typical primary cell wall surface structure. Unlike the parallel microfibrils, these macrofibrils appeared to orient randomly on the cell wall surface (Figure 4) [17].

Figure 4. High-resolution AFM height image showing a typical primary cell wall surface structure. Microfibrils are parallel-arranged, and macrofibrils scatter only on the wall surface. Scale: 200 nm.

2.2. Application in Fruit Pectin

2.2.1. Qualitative Analysis

While the primary function of AFM is to provide images of examined objects, it can be easily applied to provide qualitative information about a single macromolecule or polymer. AFM is capable of studying individual molecules so that differences in size (length, and diameter, for instance) and conformation (branch, stiffness, aggregation, association, and mode of adsorption to a substrate, for instance) between neighboring polymers can be visualized directly, thus making possible the characterization of the heterogeneity of a molecular population at the level of single polymer [2, 7, 9, 21, 40].

Figure 5 shows AFM images of sodium carbonate-soluble pectin (SSP) of peach on the 15th day under controlled atmosphere storage. Characteristic morphology of SSP can be observed from the images [33].

Pectin is an important polysaccharide in food industry that is closely related with food properties. Especially, it is closely related with the quality of fresh produce considering it is one of the most important compositions for maintaining cell wall structures of produce. AFM was used to image pectin molecules extracted from unripe tomato cell walls [26], which revealed a branched structure for tomato pectins for the first time. This branched structure differed from the neutral sugar side chains proposed from chemical analysis via enzymatic hydrolysis and sugar analysis. Later, the nature of the long branches attached to pectin molecules was investigated using AFM, which showed that the distribution and total amount of branches observed by AFM did not correspond with the pattern of neutral sugar distribution. It was postulated that the long chains consisted of polygalacturonic acid, attached to the pectin backbone through an undetermined linkage, while the neutral sugars exist as

short but undetected branches [21]. Based on the method developed for imaging individual pectin molecules, pectin polymer was later studied by AFM for addressing the detailed pectin morphology.

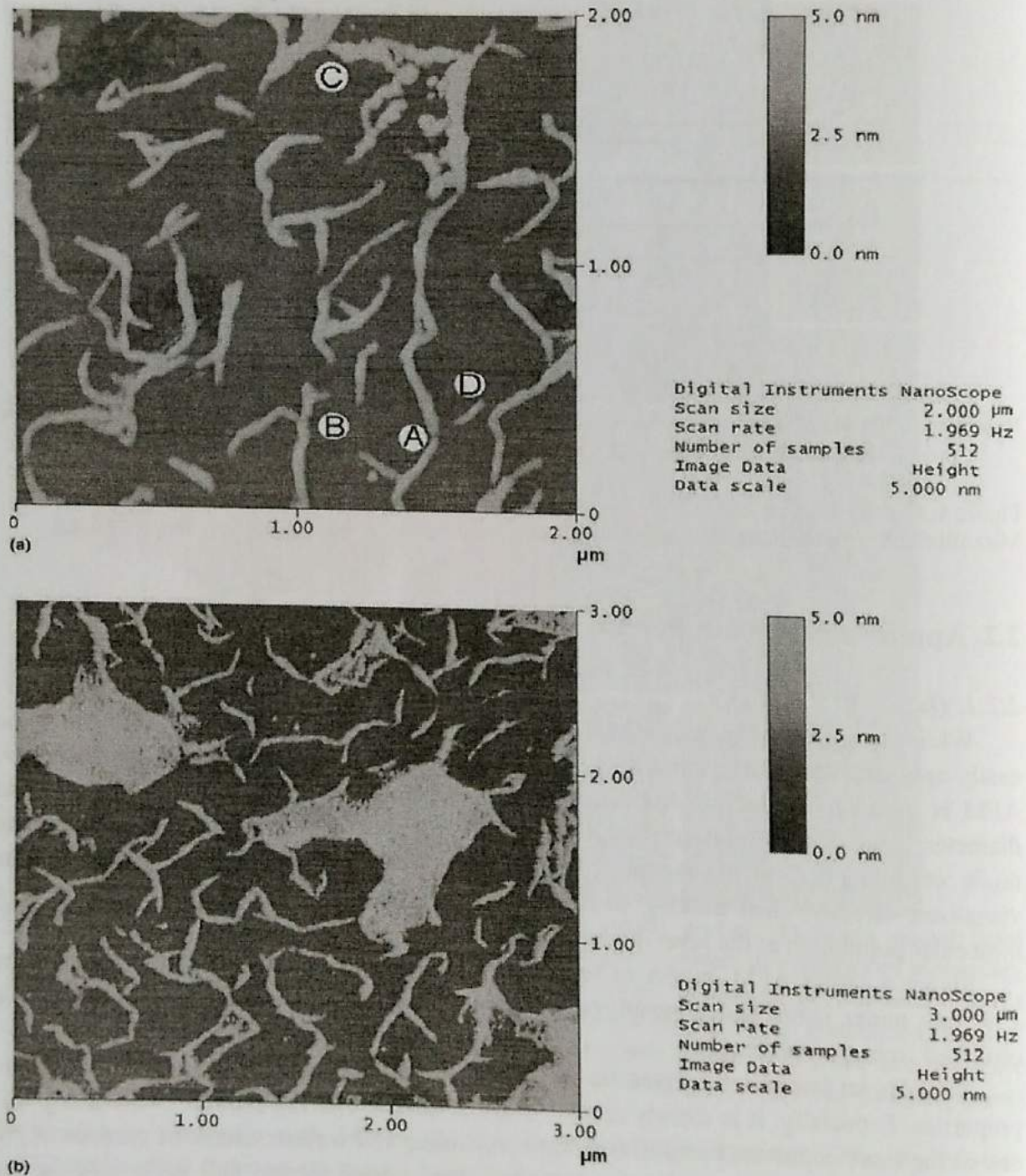

Note: A, cleavage point; B, branch; C, linear single fraction; D, polymer.

Reprinted from Food Chemistry 2006, 94, Yang H, et al., Microstructure changes of sodium carbonate-soluble pectin of peach by AFM during controlled atmosphere storage, 181, Copyright (2006), with permission from Elsevier [33].

Figure 5. AFM images of sodium carbonate-soluble pectin (SSP) of peach on the 15th day under controlled atomosphere storage. CA1: 2% O_2 + 5% CO_2, (b) CA2: 5% O_2 + 10% CO_2,

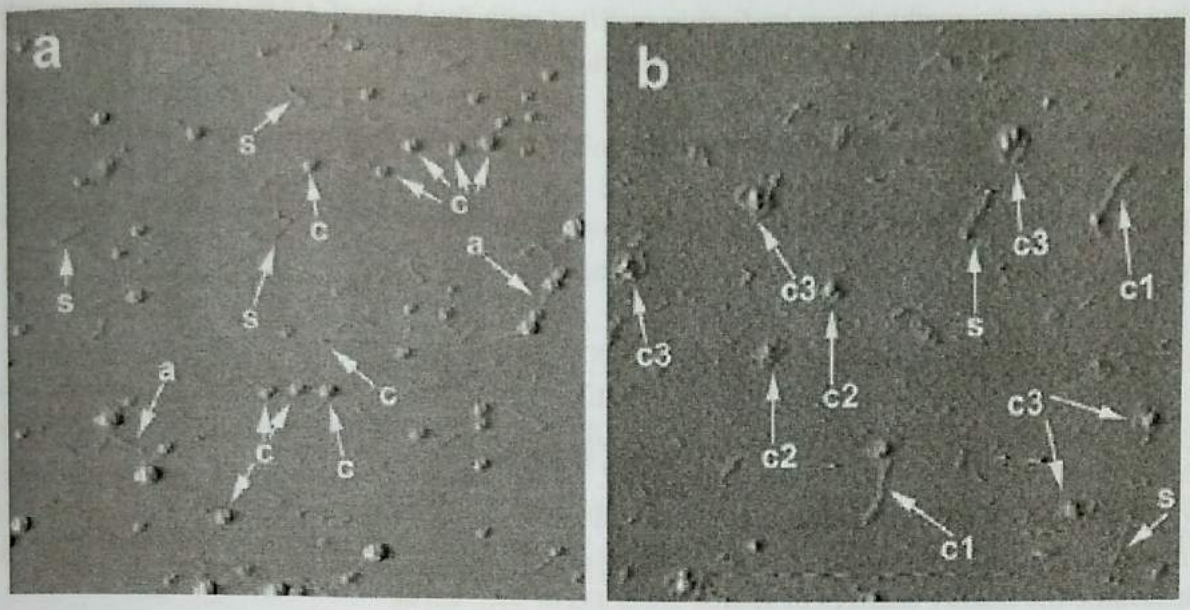

Note: image size: 1 μm × 1 μm. 's' and 'c' in the figure indicate individual extended pectin chains and protein-polysaccharide complexes, respectively. Polysaccharide-protein complexes showing individual proteins attached to one end of a pectin chain are labelled 'c1'. Examples of pectin wound tightly 'c2' and loosely 'c3' around the protein are also shown. 'a' indicates aggregates of tadpoles (polysaccharide-protein complexes).

Reprinted from Carbohydrate Polymers 2008, 71, Kirby AR, et al., Atomic force microscopy of tomato and sugar beet pectin molecules 644, Copyright (2008), with permission from Elsevier [8].

Figure 6. Error signal mode AFM images of sugar beet pectin.

Molecular interactions, especially, interactions between polysaccharides and proteins, are important for food industry [27, 28]. These interactions were successfully investigated by AFM. An example of AFM images of polysaccharides and protein complexes was shown in Figure 6. From the AFM results of sugar beet pectin, the authors suggested that there should be covalent linkages between protein and polysaccharide [8]. Two main types of aggregates were observed, with 33% of the un-aggregated molecules constituting free stiff pectin chains, labelled as 's', while 67% of the molecules being protein-polysaccharide complexes, termed as 'tadpoles' and labelled as 'c'. These protein-polysaccharide complexes exhibited three forms (noted as 'c1', 'c2' and 'c3') in Figure 6b. These results provided further testimonies supporting the idea that the extended pectin chains in contact with mica adopted a helical conformation: clearly the pectin chains wound around the proteins were much flexible. The results of the nature of protein-polysaccharide linkage would help understand the role of protein within cell wall of fruits during ripening, handling, and storage.

The heterogeneous structures of pectins and their association can be potentially resolved by high resolution AFM images. Pectin molecule has many carboxyl groups chemically, thus it can interact with the oppositely charged membranes or liposomes, leading to heterogeneous structures. Self-assembling pectin-liposome nanocomplexes (PLNs) and morphological arrangement of PLNs were characterized by AFM [34]. The attachment or association of cationic liposomes on the pectin chains forming self-assembling supramolecular complexes was visualized. A hierarchical self-assembled variety of structures, including clusters of aggregated polymer-coated particles, tubular and lamellar, or multilamellar structures were exhibited in AFM images as well. Last, macromolecular structures that were calculated from

other theoretically methods can be further testified with the help of AFM [35], which greatly expanded the use of AFM in structural elucidation.

In general, AFM imaging methodologies on different polysaccharide macromolecules and polymers share many common preparation steps and imaging parameters. These include sample preparation, scan area selection, scan rate determination, and resolution adjusting. Therefore, for imaging a new polysaccharide, researchers could refer to previous publications for imaging conditions used for other polysaccharides.

2.2.2. Quatitative Analysis

It is a great development that the quantitative parameters of samples can be investigated by AFM images. These quantitative results could provide useful information for investigating food physical and/or chemical properties. For instance, effects of polysaccharide concentration on gelling process can be quantitatively analyzed. Quantitative changes of the amount of source materials resulting in changed product morphology can be used to determine the quality changes of source materials or vice versa.

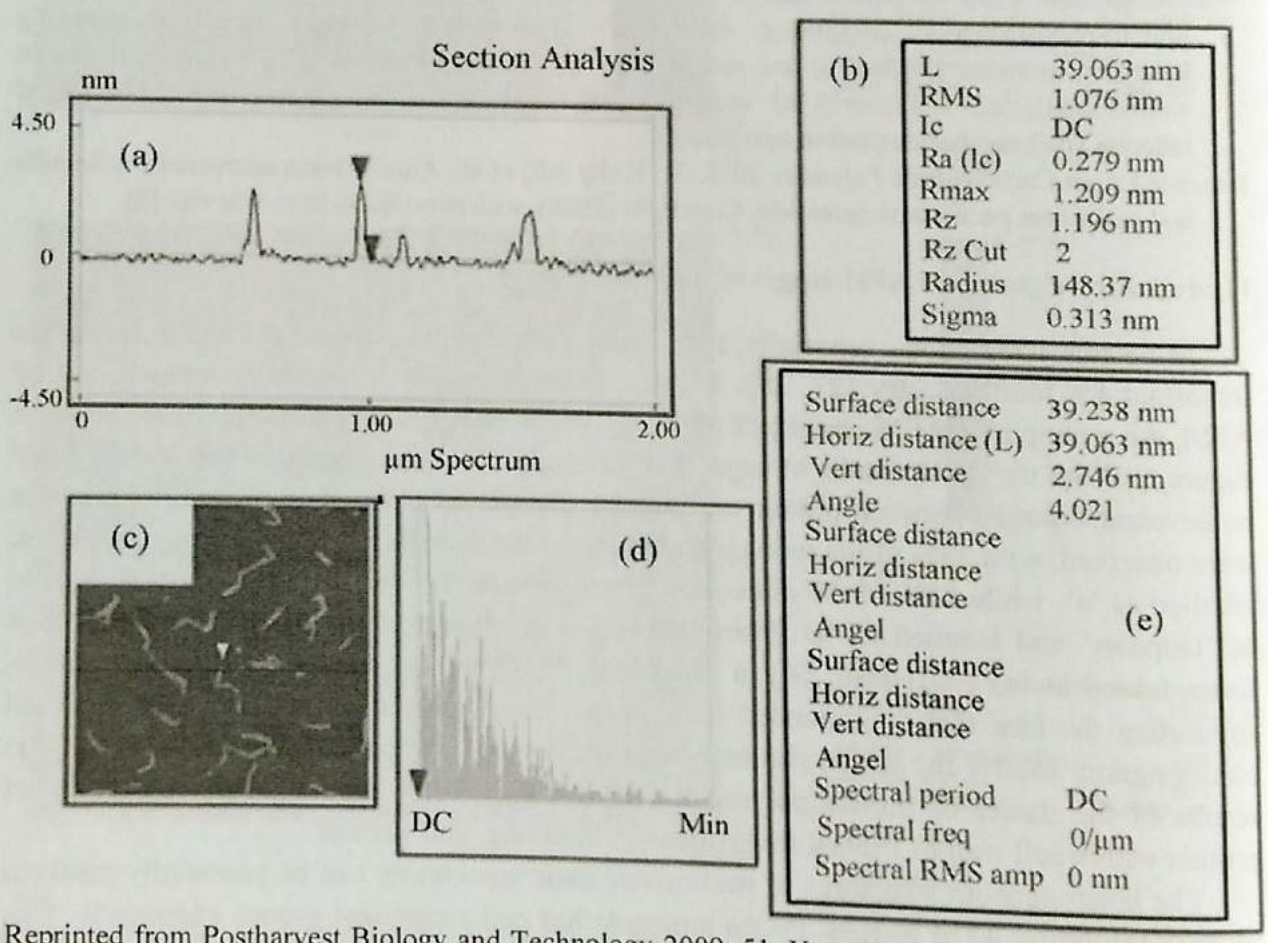

Reprinted from Postharvest Biology and Technology 2009, 51, Yang H et al., Comparative studies on nanostructures of three kinds of pectins in two peach cultivars using atomic force microscopy 396, Copyright (2009), with permission from Elsevier [39].

Figure 7. Cross-section analysis of pectin chains: (a) the height profile along across-sectional line; (b) dimension measurements of the portion of the cross-section between the two colored cursors; (c) sample of AFM image; (d) power spectrum along the cross-section; (e) dimension measurements of up to three pairs of cursors that were placed on the line section.

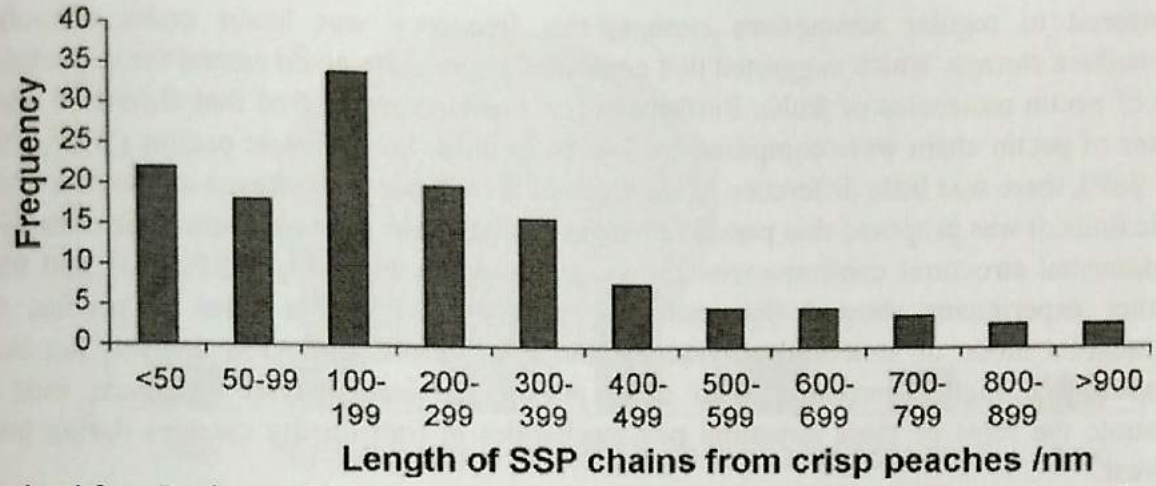

Reprinted from Postharvest Biology and Technology 2009, 51, Yang H et al., Comparative studies on nanostructures of three kinds of pectins in two peach cultivars using atomic force microscopy 396, Copyright (2009), with permission from Elsevier [39].

Figure 8. Frequencies of sodium-carbonate soluble pectin (SSP) chain lengths from the crisp peaches.

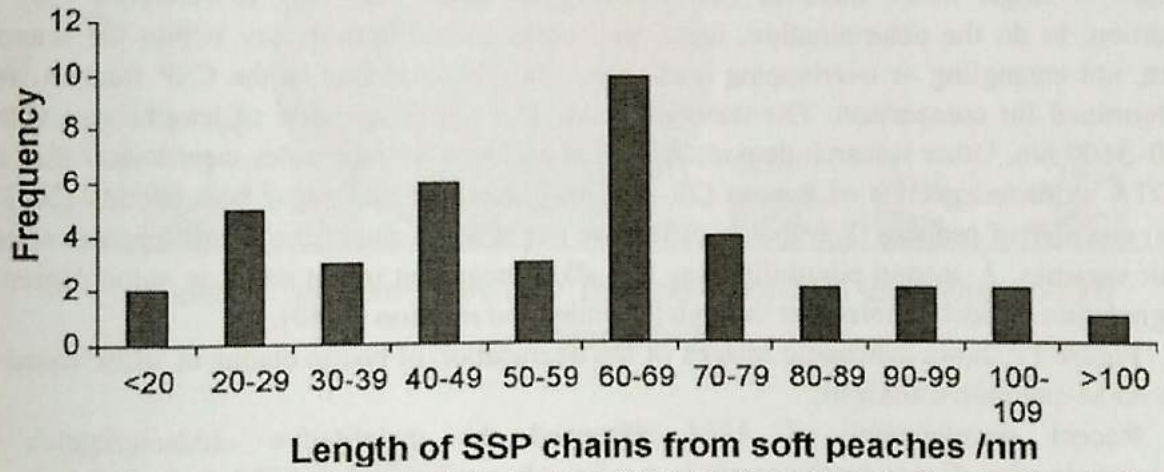

Reprinted from Postharvest Biology and Technology 2009, 51, Yang H et al., Comparative studies on nanostructures of three kinds of pectins in two peach cultivars using atomic force microscopy 396, Copyright (2009), with permission from Elsevier [39].

Figure 9. Frequencies of sodium-carbonate soluble pectin (SSP) chain lengths from the soft peaches.

AFM images explained the formation of a network in a mixture at a concentration much lower than the threshold of gellan to gel in an individual system. Gellan and xyloglucan did not form a gel at concentrations below 0.5% w/w and 0.75% w/w, respectively [36], while a mixture of 0.05% w/w gellan and 0.7% w/w xyloglucan formed a single-phase gel, indicating synergistic interactions between gellan and xyloglucan.

Quantitative parameters of AFM images for food macromolecules or polymers from different processings and storage stages were reported. The characteristics of pectin chain widths of yellow peach during storage were investigated by AFM [33, 37, 38]. Figure 7 shows a cross-section analysis of pectin chains. Figure 7c shows an AFM image of SSP from yellow peach. Quantitative data of pectin chain widths obtained from AFM images can be utilized to postulate the degradation mode of fruit pectin during post-harvest storage. Results showed that the frequency of small pectin chain widths increased with time in storage.

Compared to regular atmosphere storage, this frequency was lower under controlled atmosphere storage, which suggested that controlled atmosphere could extend the degradation rate of pectin molecules of fruits. Furthermore, it is interesting to find that almost all width values of pectin chain were composed by four basic units. For different pectins (WSP, CSP, and SSP), there was little difference in the value of these basic units. Based on the data of the basic units, it was proposed that parallel linkages or intertwists between these basic units were fundamental structural conformations for pectin molecules including WSP, CSP, and SSP. Further experiments showed that cellulose of fruits had similar rules as pectins, the degradation mode of structural polysaccharides from quantitative AFM analysis has been demonstrated highly correlated with other physicochemical analysis and been used to illustrate the roles of these structural polysaccharides in fruit quality changes during post-harvest.

Figures 8 and 9 show frequencies of SSP chain lengths from the crisp peaches and the soft peaches, respectively [39].

Figure 10 was an example of how to calculate the quantitative distribution of pectin lengths. It showed the frequencies of length of CSP single chains. The length of CSP was the length of single linear fractions (main chain) calculated according to reference [38]. In addition, to do the determination, linear molecules should entirely lay within the scanned area, not entangling or overlapping each other, only main chains of the CSP fraction were determined for comparison. The results indicate that the distribution of lengths was within 400–3600 nm. Other research demonstrated that apricot CSP molecules were longer than the CDTA extracted pectins of tomato (20–460 nm), alkali-treated sugar beet pectins (20–320 nm) and SSP of peaches [8, 39]. The difference might be resulted from the differences among fruit varieties. A second possibility was that alkali treatment might result in some degree of degradation of pectin molecules through ß-elimination reaction [8, 40].

Figure 11 shows schematic images of the degradation of pectin chains in width based on the AFM quatitative analysis.

Recent development of AFM advanced the quantitative characterization of macromolecules. Force spectroscopy is a relatively new mode of AFM that provides more quantitative information of macromolecules. It has been served as a bridge connecting nanostructure of samples with their physiochemical properties. A more recent development of AFM imaging is able to elucidate the structures and functional properties of food macromolecules simultaneously. Advanced modes of AFM imaging including phase imaging mode and force modulation mode provided quantitative results of elasticity, which can be measured from the loading and unloading force curves during AFM imaging.

While AFM is very useful for quantitative analysis, it has some limitations in quantitative determination of dimensions of macromolecules. One limitation is that during sample preparation for imaging, dehydration and lipid spreading or flattening onto the mica surface as a result of drying process may affect the actual size changes from AFM images [9].

2.3. Application in Fruit Hemicellulose and Cellulose

Hemicellulosic polysaccharide plays an important role in softening process during fruit ripening. The softening process is due to the solubilisation and depolymerisation of pectin and hemicellulose [15].

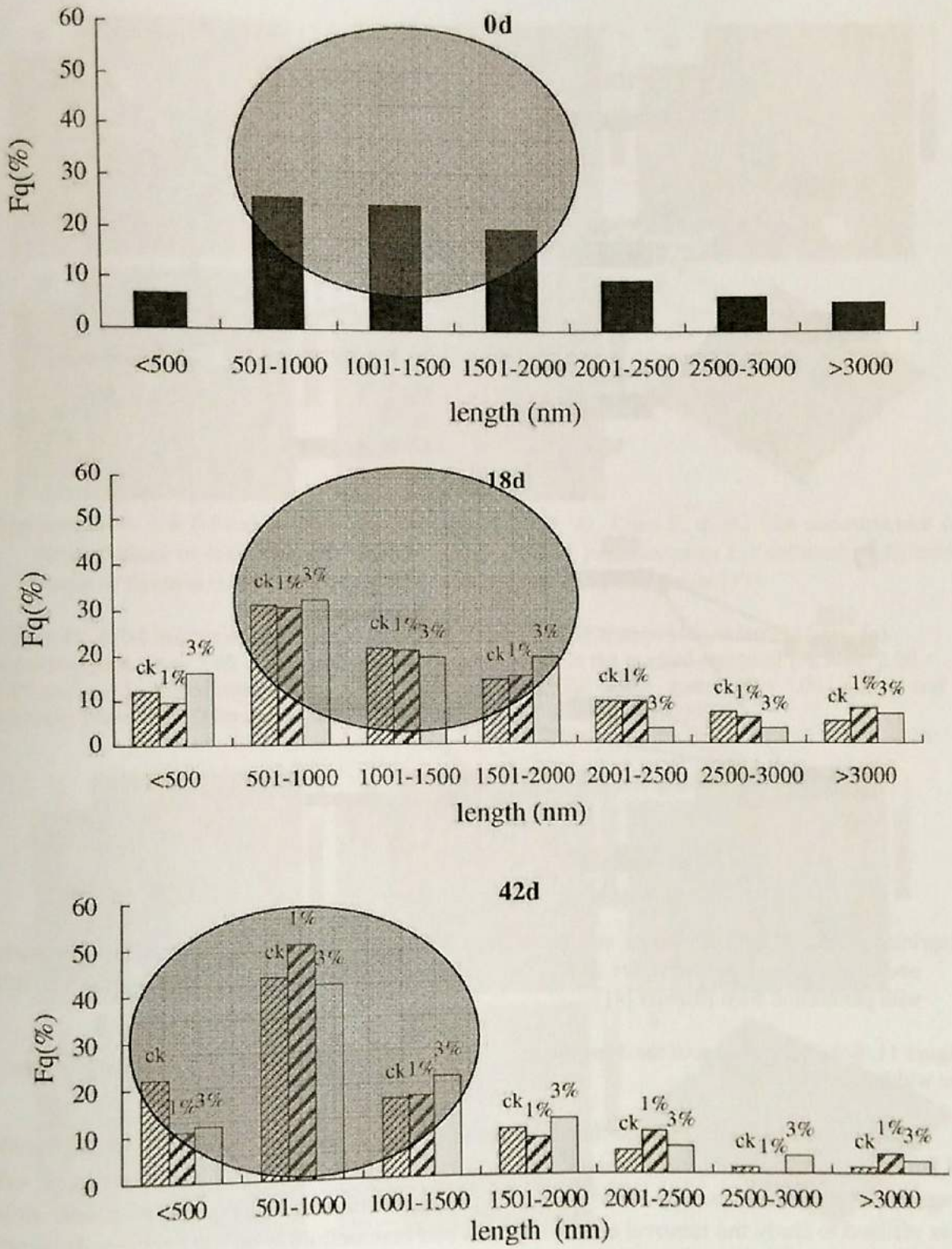

Reprinted from Food Research International 2009, 42, Liu H et al.,Effect of calcium treatment on nanostructure of chelate-soluble pectin and physicochemical and textural properties of apricot fruits 1138, Copyright (2009), with permission from Elsevier [40].

Figure 10. Length distribution of chelate-soluble pectins at harvest, on days 18 and 42 during 0 °C storage. Note. CK means control group. Groups 1% and 3% mean storage processing with 1% and 3% $CaCl_2$ solutions, respectively.

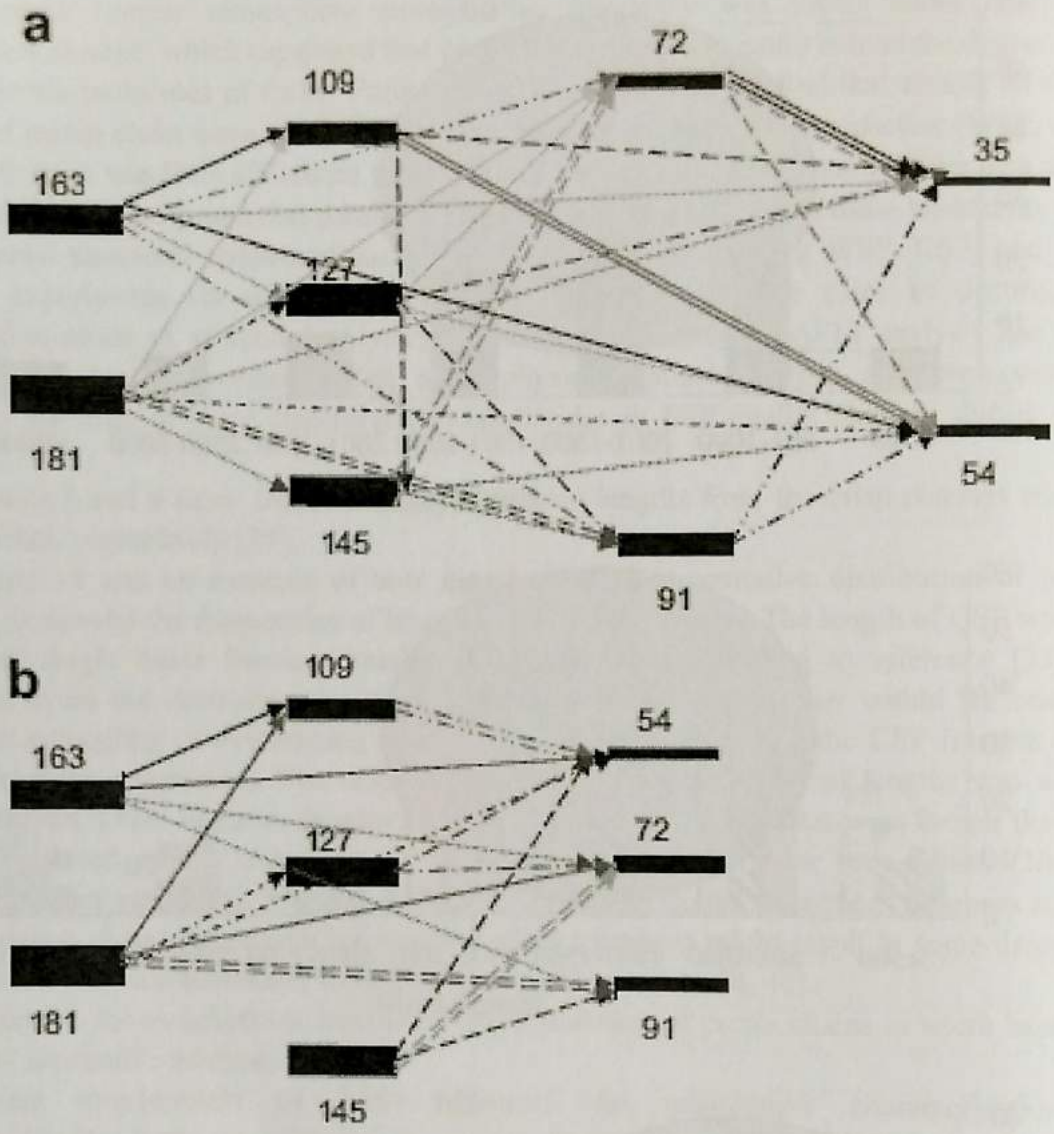

Reprinted from LWT-Food Science and Technology 2010, 43, Zhang L et al., Changes in firmness, pectin content and nanostructure of two crisp peach cultivars after storage 31, Copyright (2010), with permission from Elsevier [41].

Figure 11. Schematic images of the degradation of pectin chains in width. Note: The numbers indicate the width of pectin chains.

AFM has been used to image the cellulose networks in moist fragments of the cell walls of Bintje potato (*Solanum tuberosum L.*) [42]. Molecular structures within hydrated cell wall fragments were visualized by AFM. In addition, sequential extraction combined with AFM was utilized to study the removal effect of pectin and hemicellulose on the apparent diameters of cellulose fibers in the cell walls of onion (*Allium cepa* L.) and Arabidopsis (*Arabidopsis thaliana* L.). These studies indicated that the fibers were 4-6 nm in thickness containing single cellulose I crystals (2-3 nm in diameter) coated with non-cellulosic polysaccharides.

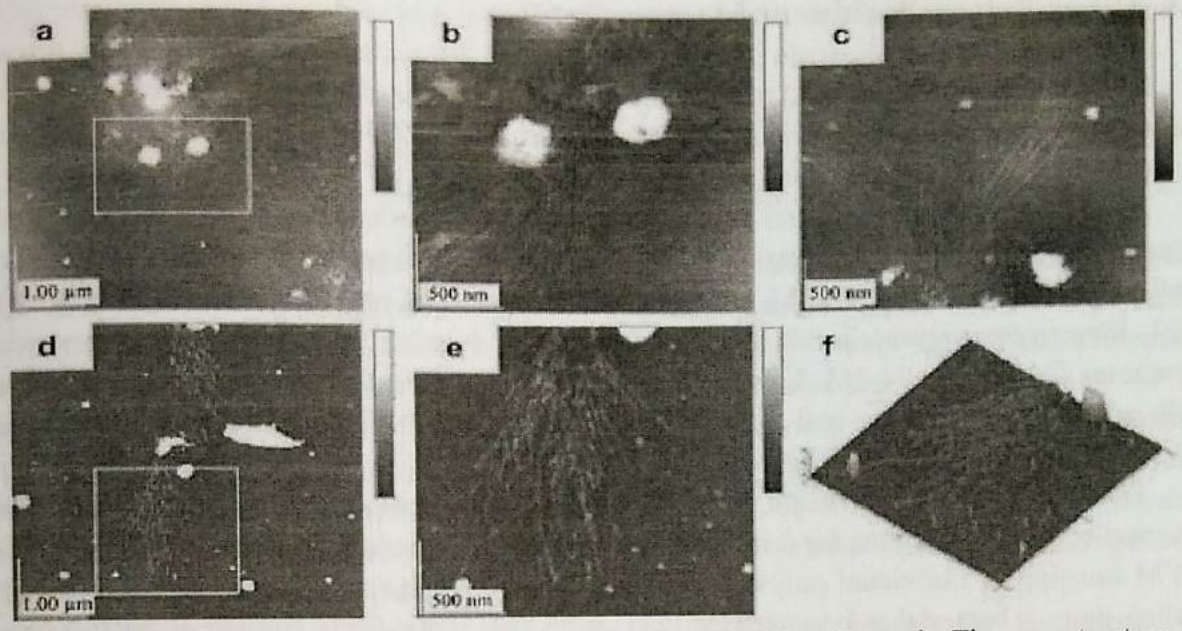

Reprinted from LWT-Food Science and Technology 2009, 42, Chen F, et al., The nanostructure of hemicellulose of crips and soft Chinese cherry (*Prunus pseudocerasus* L.) cultivars at different stages of ripeness, 128, Copyright (2009), with permission from Elsevier [15].

Figure 12. AFM images of hemicellulose from soft ripe Chinese cherry. Height bar = 15 nm. (a) atypical image, area: 5.00 × 5.00 μm^2; (b) zoom plane image in the marked region of (a), area: 2.00 × 2.00 μm^2; (c) localized image, area: 3.00 × 3.00 μm^2; (d) typical image, area: 5.00 × 5.00 μm^2; (e) and (f) zoom plane and 3D images in the marked region of (d), area: 2.00 × 2.00 μm^2.

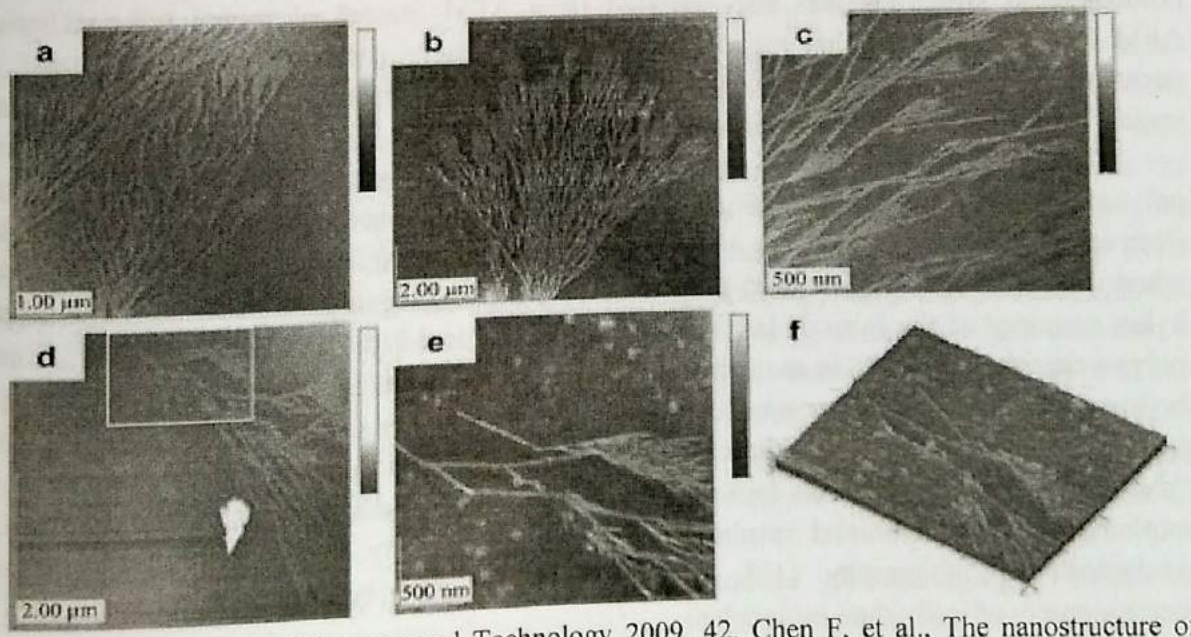

Reprinted from LWT-Food Science and Technology 2009, 42, Chen F, et al., The nanostructure of hemicellulose of crips and soft Chinese cherry (*Prunus pseudocerasus* L.) cultivars at different stages of ripeness, 128, Copyright (2009), with permission from Elsevier [15].

Figure 13. AFM images of hemicellulose from crisp ripe Chinese cherry. Height bar = 15 nm. (a) atypical image, area: 6.66 × 7.16 μm^2; (b) typical image, area: 10.00 × 10.00 μm^2; (c) localized image, area: 3.44 × 3.80 μm^2; (d) localized image, area: 7.98 × 3.97 μm^2; (e) and (f) zoom plane and 3D images in the marked region of (d), area: 2.60 × 2.11 μm^2.

2.4. Other Polysacharides or Macromolecules

In principle, almost all food macromolecules can be imaged by AFM. However, most of the current publications are about polysaccharides and proteins since there two kinds of macromolecules are so important in food science.

AFM is a relatively new and versatile technique for characterizing polysaccharides and interactions between polysaccharide and protein. The technique was applied to image cell wall polysaccharides [13, 18-21], analyze the distribution of polysaccharide contour lengths [22], investigate polysaccharide associations [23] and judge branching of polysaccharide structures [13, 18-21, 24-26]. This technique was also applied to characterize heterogeneous cell wall polysaccharides and elucidate the role of starch-binding domains in digesting crystalline starch by glucoamylase [27, 28].

To date, AFM has been used to image individual macromolecules and their intermolecular associations for dozens of years [16, 23]. A method was developed in 1996 for AFM imaging of individual polysaccharides in order to image networks and gels formed by gellan gum, a bacterial polysaccharide [23]. With this method, the surface of bulk aqueous gellan gels can be imaged both under butanol and in air. Compared to imaging in air, imaging in alcohol has the advantage of significantly reducing the shear force between the tip and the sample, which will help maintain the sample intact. However, a disadvantage of imaging in alcohol is that alcohol may affect samples, for instance, if the sample is polysaccharide, alcohol may precipitate the polysaccharide and change the gel structure [29]. Reports of AFM images of iota carrageenan indicated that the network formed by refined iota carrageenan was homogeneous and composed by a continuous branched polymer [30]. This similar kind of homogeneous structures was also reported from AFM images of monoi polysaccharides. AFM images indicated that monoi polysaccharides were composed of linear chains and occasional long branches. The distribution of molecular weight was wide with large variability in end-to-end lengths along single chains [31].

AFM can also be used to elucidate different aggregation modes for different polysaccharides, providing additional information that is beneficial to the results obtained from other instruments. By using AFM, researchers found that hyaluronan networks dispersed when diluted, showing individual molecules or small aggregates, while at the same dilution hylan remained as the form of large aggregates [32]. In addition, AFM can be used to record polysaccharide molecules in motion [19]. Therefore, different forms appearing with time can be imaged and recorded. For a water-soluble wheat pentosan, different forms of loops, trains and tails were confirmed from direct imaging by AFM. The formation of linear and entangled "shoe-lace" shaped structures, two of the most common appearances for arabinoxylans, was explained by the combined results from AFM morphology, chemical analysis and size-exclusion chromatography [13]. Moreover, AFM can be used to characterize the heterogeneity of individual molecules.

Based on the methods developed for polysaccharides from plant and animal sources, more researchers have explored the methods for characterizing the polysaccharides extracted from commonly used food materials. Starch is a major food component, which is widely applied as a source material for many foods in food processing. When hot amylose solutions were incubated with iodine and Tween-20 (a non-ionic surfactant) to stabilize the amylose molecules, and examined by AFM, the sample exhibited a distribution of extended chain-like

molecules from AFM images, and they directly visualized some branched macromolecules for the first time [24]. Some branched macromolecules were observed for the first time.

2.5. Characterization of Fruit Surface

AFM has become a standard tool for characterizing the heterogeneity at nano scale, being applied in almost every aspect of surface and interface sciences [5, 43]. AFM is a powerful instrument for qualitatively determining roughness and other surface characteristic parameters. Some tiny features of the surface can be investigated and characterized by AFM. Topographical and frictional investigations using AFM are able to measure surface characteristics including roughness, homogeneity, surface morphology and fractal analysis. For biological samples, the surface characteristics also involve interactions (forces) generally called colloidal forces, including electrostatic interactions, steric interactions and specific adhesion forces at molecular contact.

Researchers have realized the importance of developing sensors for nondestructive assortment in real-time mode AFM. Fine structure of onion skin was studied and the surface roughness of alginate-coated onion skin and the control group was compared using AFM [44]. Results indicated that the smoother the alginate-coated samples were, the lower the roughness values were obtained from AFM. Similar results were reported for garlic [45]. Yang and others (2005) used AFM roughness analysis to characterize the surface status of fresh and stored fruits and vegetables [46]. They found that with the increase of storage time, the roughness value was found increased. Figure 14 shows profiles of peach skin at initial storage by AFM.

The authors also pointed out a limitation of their study, which was relatively small scanned areas, thus it was hard to use the results to indicate the surface status of the whole sample. Similar shortcomings were found from other reports [44], with scan area less than 250 μm^2. In addition to the small scammed area, another potential shortcoming was the influence of the possible vasculature part of the sample surface. A third shortcoming for direct imaging the surface of produce was that it might result in stain of the AFM tip when imaged in air, thus affecting the result of next imaging, and resulting in inaccurate roughness of the produce surface [46]. A solution for this was developing scanners which can scan a large area and imaging in solution for decreasing the force between the AFM tip and the sample surface. In this case, the image areas can be significantly increased and contamination of the tip reduced, the roughness results obtained from AFM would be more reliable and accurate, being able to serve as an indicating index for appearance quality of produce in commerce.

For some characterization of the surface of fresh produce, phase imaging AFM can be applied. It is powerful for characterizing complex surfaces, mapping surface friction and adhesion, and finding surface contamination. For maize starch films, phase imaging provided detailed smooth and rough domains, which were not approachable by height mode imaging. Considering AFM can characterize the delicate food surface at the micro or nano scale, it could be applied to investigate the effects of edible coatings on fresh produce.

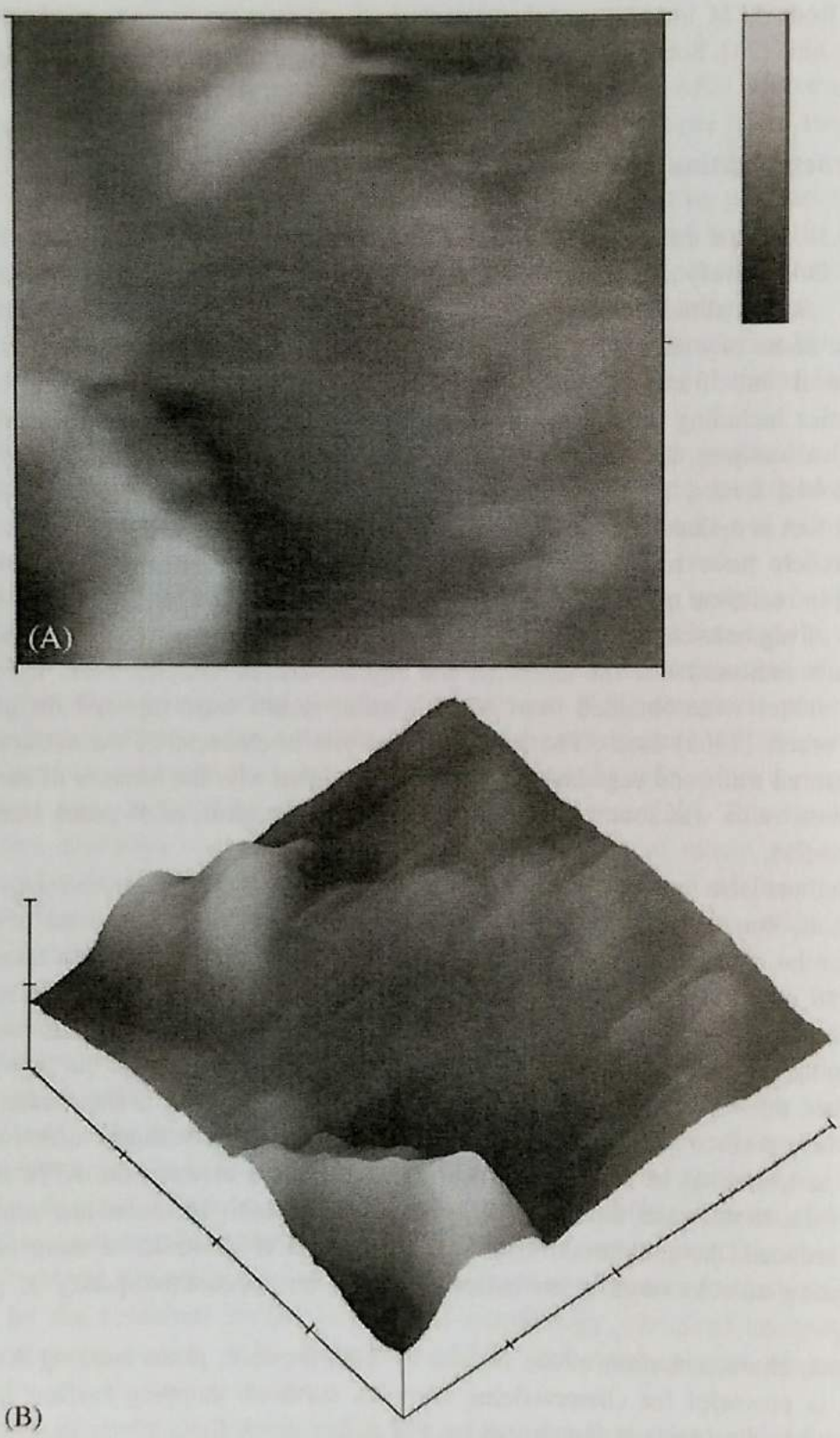

Reprinted from LWT-Food Science and Technology 2005, 38, Yang H, et al., Visualization and quantitative roughness analysis of peach skin by atomic force microscopy under storage, 38. Copyright (2005), with permission from Elsevier [46].

Figure 14. Profiles of peach skin at initial storage by AFM: (A) plane profile and (B) three-dimensional profile. Scan area = 1.999 μm × 1.999 μm, height bar = 50 nm.

2.6. Manipulation of Fruit Polysaccharides

Many food macromolecules have tangled structures. Therefore, they generally form curly chain structures during their solidifying on the support, mica surface, for instance. Take pectin for instance, the aggregation of pectin chains takes place during preparation of the pectin sample on the mica surface before scanning, which might cause the potentially measurable molecular characteristics being unmeasurable. In addition, due to their heterogeneous structures, pectin molecules generally have varied structures or complex repeat units, which would make them tend to be averaged over the whole sample with most current methods.

AFM, however, is capable of studying individual molecules adsorbed onto surfaces without complex preparation or other agents added. Based on current reports, visualization of pectin structure is easy to attain by AFM. However, considering pectin molecules often associate with each other, it is hard to get exact dimensional information of their chains. Manipulation of molecules provides an opportunity to measure individual food molecules or interactions between different food macromolecules directly [7]. Only after pectin manipulation such as stretching into a line can other important related information including branching structure of pectin, molecular mass distribution, and degradation mode of chain widths and lengths with time be elucidated accurately based on pectin morphology analysis.

Recently, with the increased interests of researchers in nanotechnology, molecular manipulation at nano scale has become an interesting scientific topic. Currently reported manipulation on macromolecules mainly belongs to two strategies. One is at the stage of sample preparation before AFM imaging, which is based on two commonly used methodologies: molecular combing, and fluid fixation including gas flow. The other is manipulation using special tip which can interact with the sample for attaining manipulation during scanning. An example for this is lateral-interchange atomic manipulation with AFM [47]. To date, most of food biomaterials related manipulation belongs to the first category.

Manipulation of food macromolecules has wide applications in the field of food science and technology. For instance, manipulation of pectin molecules can be used to investigate the effects of pectins on food properties and the concrete changes of pectins themselves during food processing and handling. Stretching pectin molecules will make it possible to determine the lengths of the molecules. Manipulation including molecular combing and fluid fixation techniques is able to position, stretch, and align individual pectin molecules, making pectin aggregates extended, and the interaction between pectin molecules and others observable [7].

Figures 15 and 16 show the effects of manipulation on CSP and SSP from peaches, respectively. In the two Figures, pectin molecules on mica surfaces, aligned and stretched by manipulation methods, were imaged in air with AFM. Within the two methods of molecular combing and fluid fixation, modified molecular combing was more effective in molecular manipulation than fluid fixation technique. By molecular combing, CSP was straightened into lines in one direction while SSP was stretched into 'V' shape. Schematic images indicated the processing for the two pectins (Figure 17).

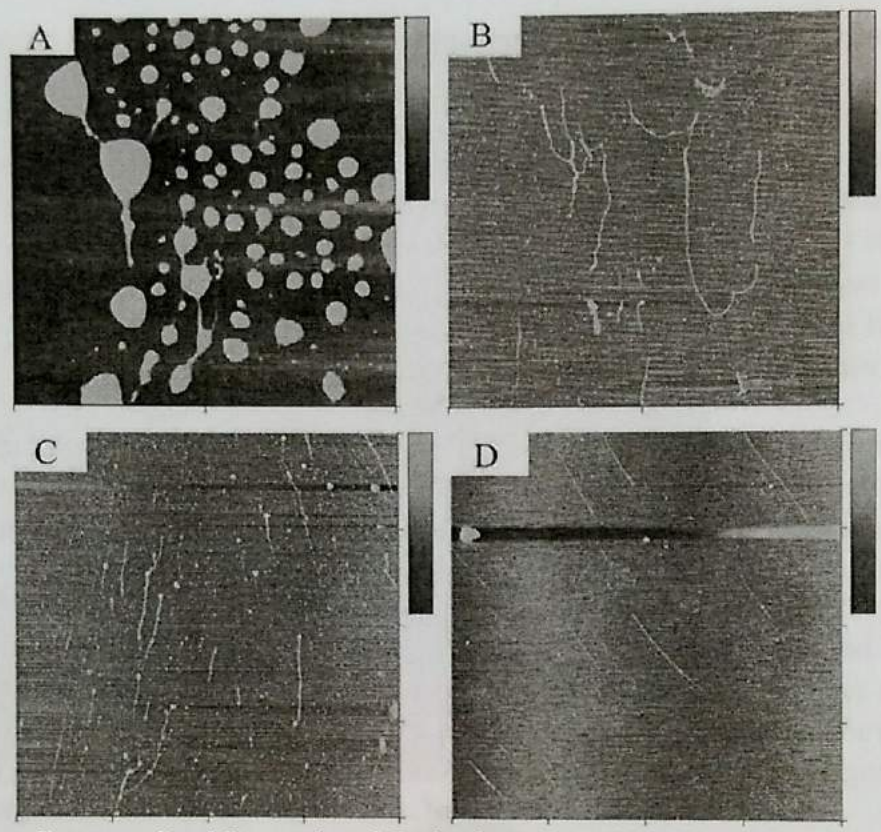

Reprinted from European Food Research and Technology 2006, 223, Yang H, et al., Manipulate and stretch single pectin molecules with modified molecular combing and fluid fixation techniques 80, Copyright (2006), with permission from Springer [7].

Figure 15. AFM images of effects of manipulation on the chelate-soluble pectin from peaches. Height *bar*: 2 nm. (A) typical image without manipulation, image size: 5.0×5.0 μm. (B) untypical image without manipulation, image size: 5.0×5.0 μm. (C) image after fluid fixation manipulation, image size: 10.0×10.0 μm. (D) image after modified molecular combing manipulation, image size: 10.0×10.0 μm.

3. Relationship between Polysaccharide Morphology and Fruit Physicochemical Analysis

3.1. Pectin Structural Determination from Biochemical Analysis

Pectin, hemicellulose, and cellulose are three major polysacchrides related to fruit mechanical properties. Elucidation of their chemical changes as well as morphological changes is beneficial to maintaining fruit quality.

Walls of growing fruits are very complex and sophisticated, containing materials of polysaccharides, proteins and other components incorporating into a dynamic assembly. Among the polysaccharides, pectins are composed of many acidic heteropolysaccharides; they associate into a repertoire of structural complexity with at least three domains. Most of these domains are known for their structural heterogeneity. Ramnogalacturonan II (RG-II) is one of the domains, which exhibits a remarkable conservation among almost all fruits. RG-II is viewed as the most complex plant polysaccharide, playing a major role in maintaining structure and growth of fruits (15)

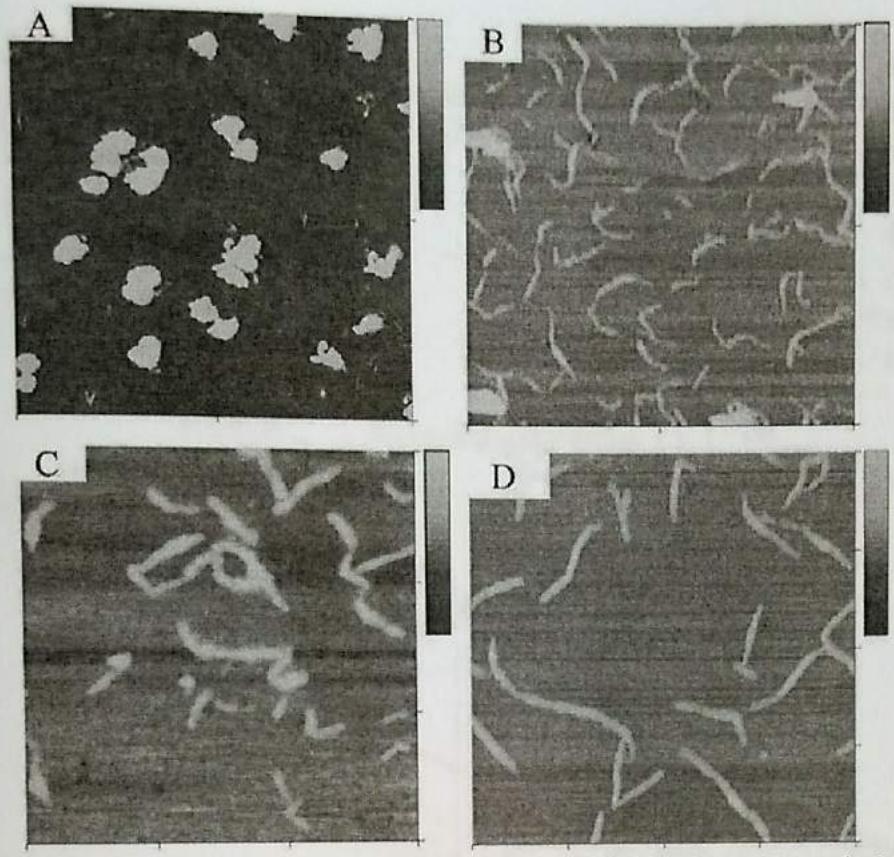

Reprinted from European Food Research and Technology 2006, 223, Yang H, et al., Manipulate and stretch single pectin molecules with modified molecular combing and fluid fixation techniques 81, Copyright (2006), with permission from Springer [7].

Figure 16. AFM images of effects of manipulation on the sodium carbonate-soluble pectin from peaches. Height bar: 5 nm. (A) typical image without manipulation, image size: 5.0×5.0 μm. (B) untypical image without manipulation, image size: 2.0×2.0 μm. (C) image after fluid fixation manipulation, image size: 1.5×1.5 μm. (D) image after modified molecular combing manipulation, image size: 1.0×1.0 μm.

By the presence of a "wall", plant cells are distinguished from animal cells. Within the wall, physicochemical and enzymatic processes take place. During cell growth, the first wall deposited after cell division is named as "middle lamella", which is basically composed of pectins [48]. The cell then forms a wall composed of "primary" cell wall to supplant the "middle lamella". The primary cell wall is a glycolproteinaceus layer, composed of proteins and polysaccharides including pectin, hemicellulose, and cellulose [15]. These polysaccharides are notable for their structural heterogeneity. Fruit tissue has evolved complex structural and chemical mechanisms for resisting attack on its structural sugars from microorganisms and animals [49]. Take cellulose for instance, at molecular level, the crystalline cellulose core of cell-wall materials is highly resistant to chemical and biological hydrolysis because of its structure [50]. In a cellulose sheet, there are strong interchain hydrogen bondings between adjacent chains, while between cellulose sheets, there is relatively weak hydrophobic interactions. The strong interchain hydrogen-bonding network causes crystalline cellulose much resistant to enzymatic hydrolysis [50], while hemicellulose and amorphous cellulose are easily to be digested [49].

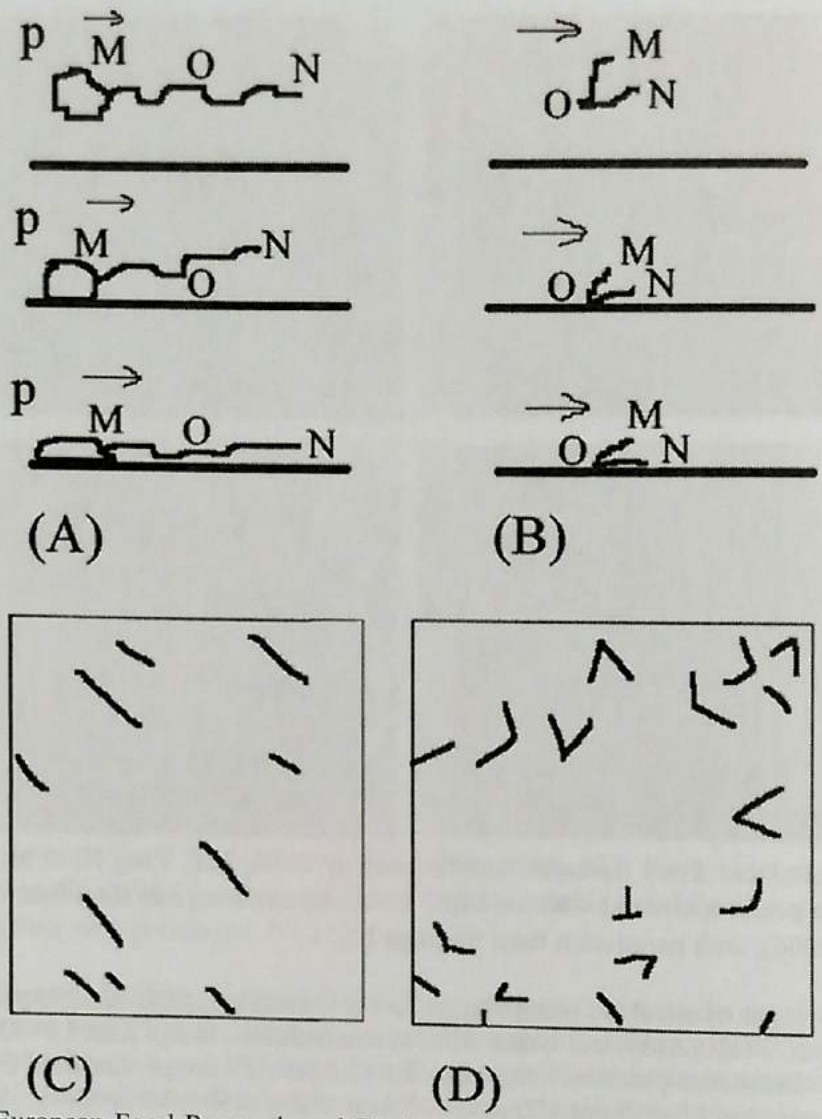

Reprinted from European Food Research and Technology 2006, 223, Yang H, et al., Manipulate and stretch single pectin molecules with modified molecular combing and fluid fixation techniques 82, Copyright (2006), with permission from Springer [7].

Figure 17. Schematic images of theoretical and practical manipulation and aligning of the pectin molecules. **A** possible stretching pathway of chelate-soluble pectin molecules. **B** possible stretching pathway of sodium carbonate-soluble pectin molecules. **C** scheme of chelate-soluble pectin alignment after modified molecular combing manipulation. Image size: 10.0×10.0 μm. **D** scheme of sodium carbonatesoluble pectin alignment after modified molecular combing manipulation. Image size: 1.0×1.0 μm. Note: P, means chelator, CDTA; M, N, mean end points of pectin molecular chain; O, means the middle point of pectin chain.

Figure 18 shows a schematic image representation of the primary structure of pectins [51].

AFM images of monomer mRG-II and dRG-II are shown in Figure 19.

The profiles in Figure 19 presented broad peaks in both images, which made it difficult to compare each other. However, extension peaks from dRG-II were found twice higher than those obtained for monomer. The results agreed with a model of two flattened disks stacked on top of each other. It provides a good example of chemcial analysis compatible with morphology results.

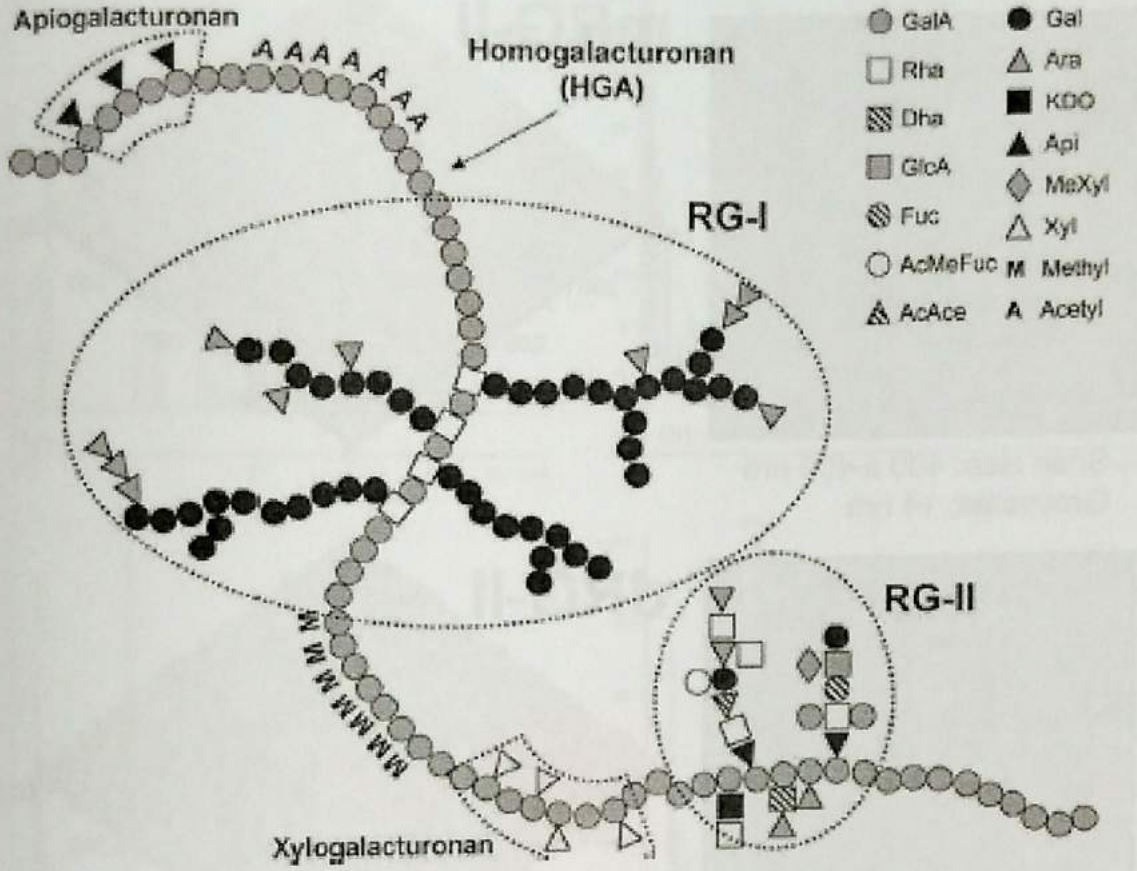

Reprinted from Biochimie 2003, 85, Perez S, et al., A complex plant cell wall polysaccharide: rhamnogalacturonan II. A structure in quest of a function, 110, Copyright (2003), with permission from Elsevier [51].

Figure 18. Schematic representation of the primary structure of pectins.

Table 2. Neutral sugar compositions (mg/100 g) of tomato CSP in two cultivars and two ripening stages [e]

Monosaccharide	Unripe 'Dongsheng'	Ripe 'Dongsheng'	Unripe 'Geruisi'	Ripe 'Geruisi'
Man	0.92±0.27b	1.02±0.04b	1.59±0.06a	0.99±0.13b
Rib	0.51±0.19a	0.45±0.09a	0.48±0.11a	0.62±0.06a
Rha	1.37±0.35c	2.62±0.45ab	2.01±0.29b	2.73±0.03a
GlcUA	0.40±0.06b	0.49±0.09ab	0.63±0.07a	0.48±0.13ab
GalUA	15.14±3.40b	22.93±0.35a	14.74±0.39b	15.84±0.56b
Glc	4.04±0.09b	3.64±0.09c	4.35±0.10a	3.78±0.10c
Gal	3.42±0.46b	3.92±0.37b	6.03±0.47a	4.05±0.73b
Xyl	1.65±0.04c	2.76±0.53b	3.45±0.21a	1.91±0.41c
Ara	2.02±0.32b	2.70±0.57a	3.03±0.06a	2.50±0.19ab

[e] The values that have different letters in the same line are significantly ($P < 0.05$) different.

Reprinted from Food Chemistry 2010, 121, Xin Y, et al., Morphology, profile and role of chelate-soluble pectin on tomato properties during ripening, 376, Copyright (2010), with permission from Elsevier [53].

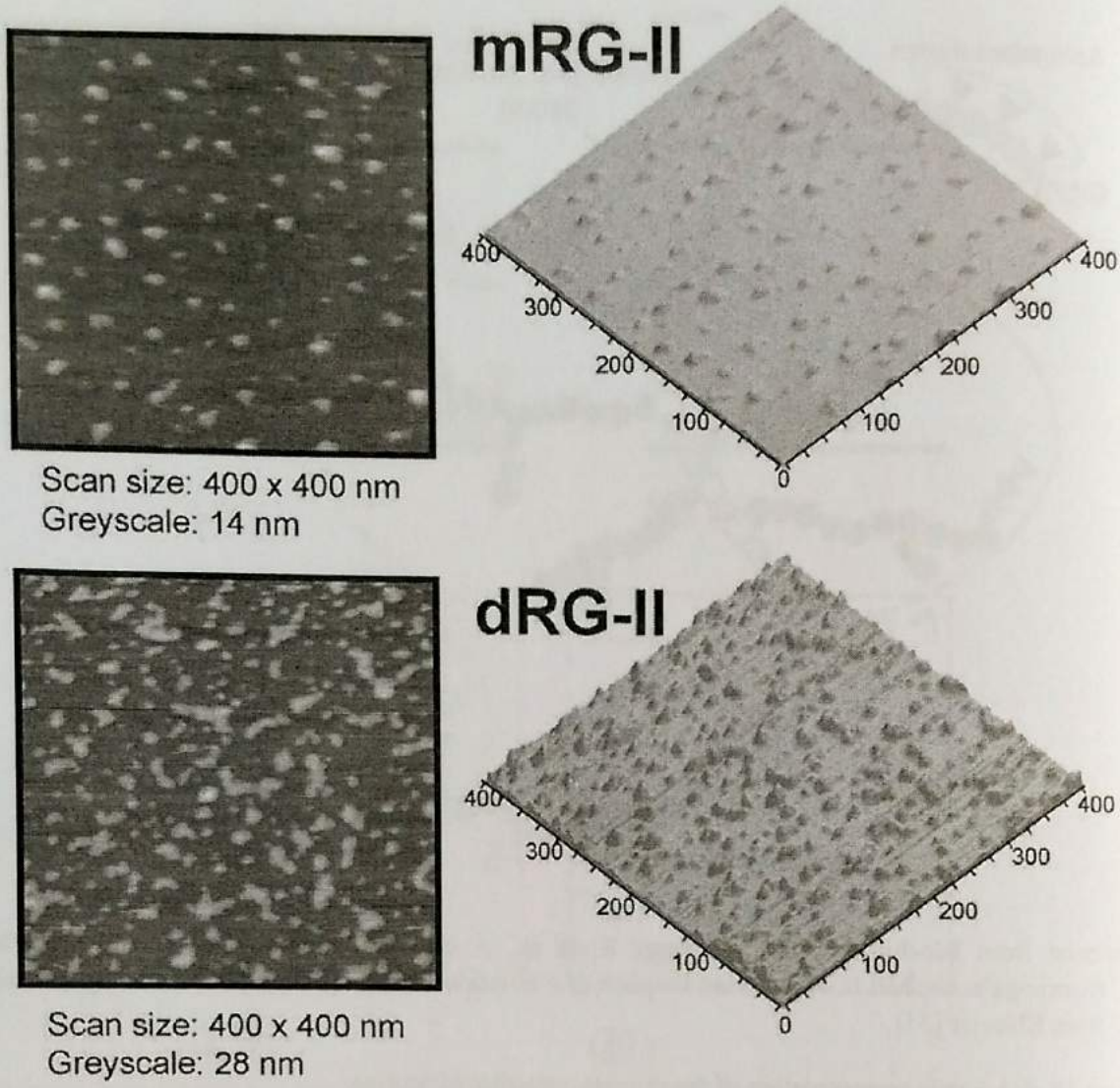

Reprinted from Biochimie 2003, 85, Perez S, et al., A complex plant cell wall polysaccharide: rhamnogalacturonan II. A structure in quest of a function, 117, Copyright (2003), with permission from Elsevier [51]

Figure 19. AFM images (left) and pseudo-3D-images generated from greyscale (right) from mRG-II (monomeric) and dRG-II (dimeric). The samples were diluted (1–10 μg/ml) and 2 μl were deposited onto freshly cleaved mica and allowed to dry in air. The samples were imaged in a liquid cell under butanol in dc contact mode under constant force conditions (method taken from [52]).

AFM morphology can be combined with chemical determination by HPLC to elucidate the evolution of sugar components of fruits during storage [53]. Figure 20 shows the profiles of HPLC analysis of monosaccharides from tomato CSPs. Quantitative results are shown in Table 2.

3.2. Pectin Mechanical Properties by AFM Analysis

It has been well established that textural changes are largely determined by fruit cell wall and middle lamella polysaccharides. Cell wall polysaccharides mainly include pectin, hemicellulose and cellulose.

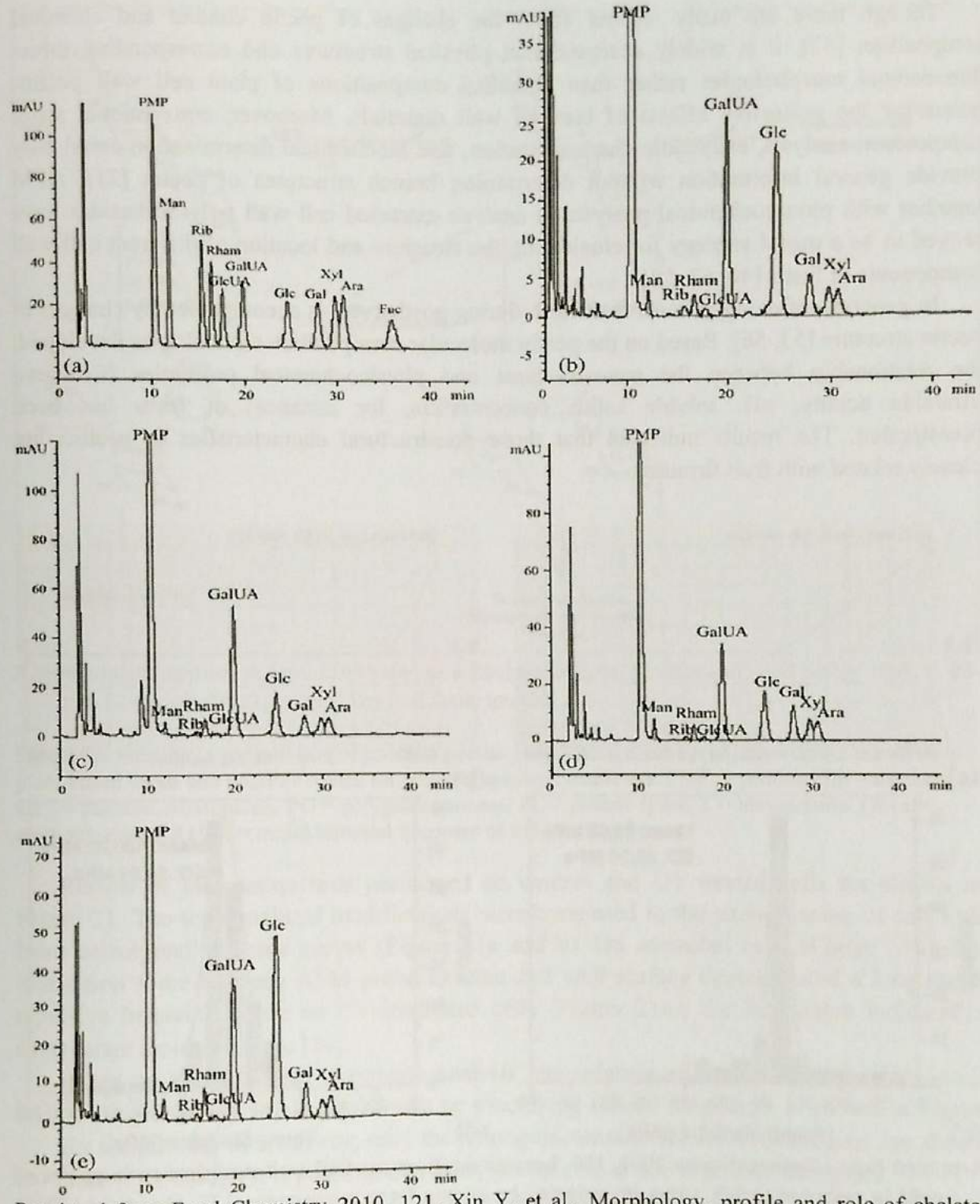

Reprinted from Food Chemistry 2010, 121, Xin Y, et al., Morphology, profile and role of chelate-soluble pectin on tomato properties during ripening, 375, Copyright (2010), with permission from Elsevier [53].

Figure 20. HPLC images of monosaccharides from tomato CSPs (Sugars are expressed as Man, Mannitose; Rib, ribose; Rha (Rham), rhamnose; GlcUA, glucuronic aicd; GalUA, Galacturonic acid; Glc, glucose; Gal, galactose; Xyl, xylose; Ara, arabinose; Fuc, fucose.). (a) Ten standard monosaccharides; (b) 'Dongsheng' turning stage tomato; (c) 'Dongsheng' light-red stage tomato; (d) 'Geruisi' turning stage tomato; and (e) 'Geruisi' light-red stage tomato.

Though there are many reports about the changes of pectin content and chemical composition [57], it is widely accepted that physical structures and corresponding three-dimensional morphologies rather than chemical compositions of plant cell wall pectins determine the protective effects of the cell wall materials. Moreover, conventional sugar composition analysis, enzymatic characterization, and biochemical determination could only provide general information without determining branch structures of pectin [21]. AFM together with physicochemical analysis to analyze extracted cell wall polysaccharides have proved to be a useful strategy for elucidating the structure and location of different cell wall components of fruits [40, 53, 58].

In general, softening of most fruit flesh during postharvest is accompanied by changes of pectin structure [53, 56]. Based on the pectin molecular manipulation technologies developed, the relationship between the nanostructures and physicochemical properties (firmness, titratable acidity, pH, soluble solids concentration, for instance) of fruits has been investigated. The results indicated that those nonstructural characteristics of pectins are closely related with fruit firmness.

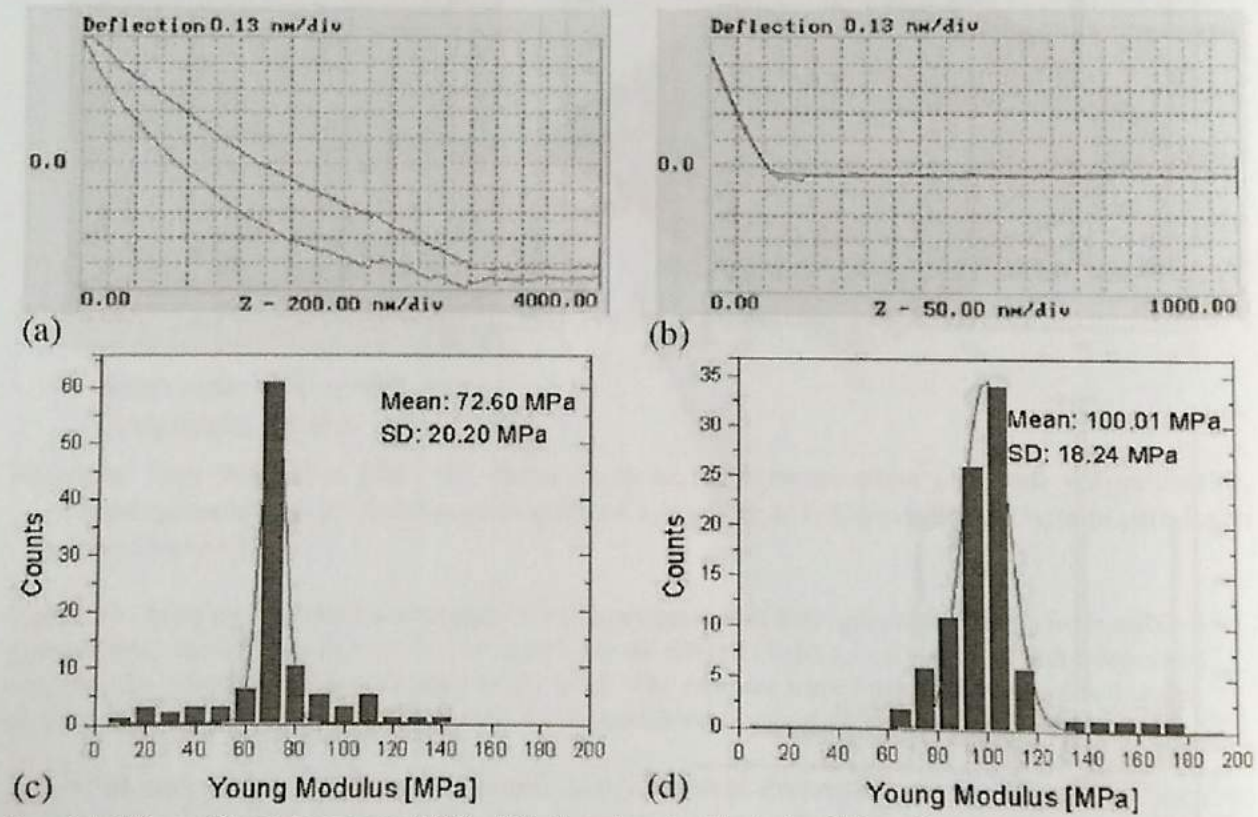

Reprinted from Ultramicroscopy 2004, 100, Lesniewska E, et al., Cell wall modification in grapevine cells in response to UV stress investigated by atomic force microscopy, 177, Copyright (2004), with permission from Elsevier [54].

Figure 21. Evolution of the cell wall mechanical properties. (a) Typical deflection curve on untreated cells showing long-range repulsive force. (b) Typical deflection curve on UV-treated cells taken 3.5 h after elicitation in Nitch–Nitch medium showing short-range repulsive force. The corresponding measured elastic moduli on Gamay cells, based on an assumed Poisson ratio of 0.3, ranged from 72 MPa for untreated cell walls (c) to 100 MPa for UV-treated cell walls (d).

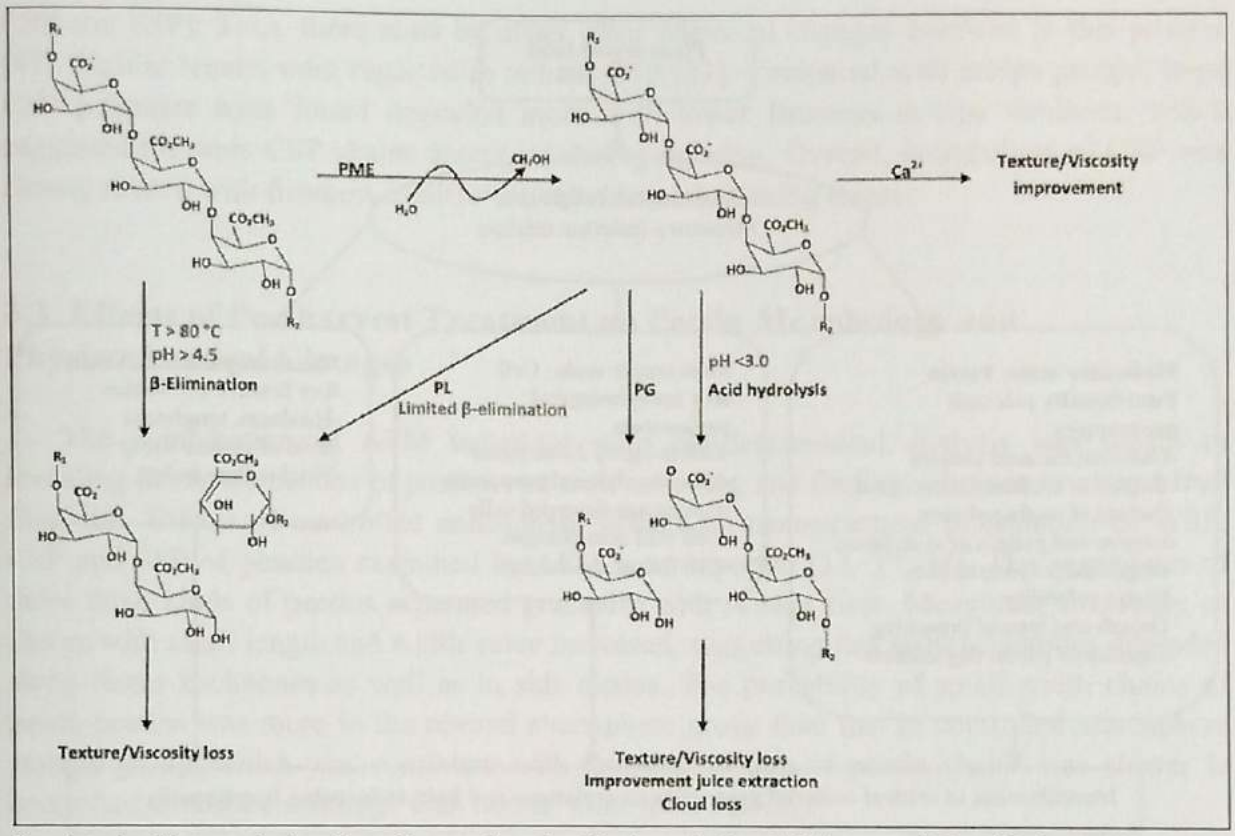

Reprinted with permission from Comprehensive Reviews in Food Science and Food Safety 2009, 8, 86-104. Copyright (2009), John Wiley and Sons, Inc [55].

Figure 22. Schematic presentation of possible pectin (only homogalacturonan) conversion reactions in plant-based foods and possible routes for tailoring quality parameters: PME = pectinmethylesterase, Ca^{2+} = calcium crosslinking, PG = polygalacturonase, PL = pectate lyase, T = temperature, OMe = methoxy-esters, R1/R2 = initial/terminal fragment of the pectin polymer.

Results of indentation tests performed on control and UV-treated cells are shown in Figure 21. The topographical modifications were correlated to the strengthening of cell wall from corresponding force curves (Figure 21a and b). On untreated cells (Figure 21a), the interaction force between AFM probe and the cell wall surface demonstrated a long-range repulsive behavior, while on UV-irradiated cells (Figure 21b), the interaction indicated a short-range repulsive force [54].

Based on chemical and enzymatic analysis, degradation of fruit pectin by endogenous and/or exogenous enzymes, postharvest or processing related treatments is shown in Figure 22. For simplifying the pathway, only the homogalacturonan conversion reactions are shown in Figure [55], though it is possible that many pectin conversion reactions take place.

Many studies on the effect of pre-processing or processing conditions on the mechanical properties of plant-based foods are empirical-based. It is widely accepted that structure-function relationship touches three levels of fruits: molecular scale, mesoscopic scale, and macroscopic scale. Figure 23 shows the correlations between pectin changes in situ micro- and macromechanical properties of plant-based food, fruit, for instance (35). From Figure 23, it is obvious that chemical and morphological analyses play key roles in the assessment of food quality, from current reports, research at molecular scale mainly relies on chemical analysis, AFM morphology analysis would greatly expand the knowledge about quality related properties of fruits.

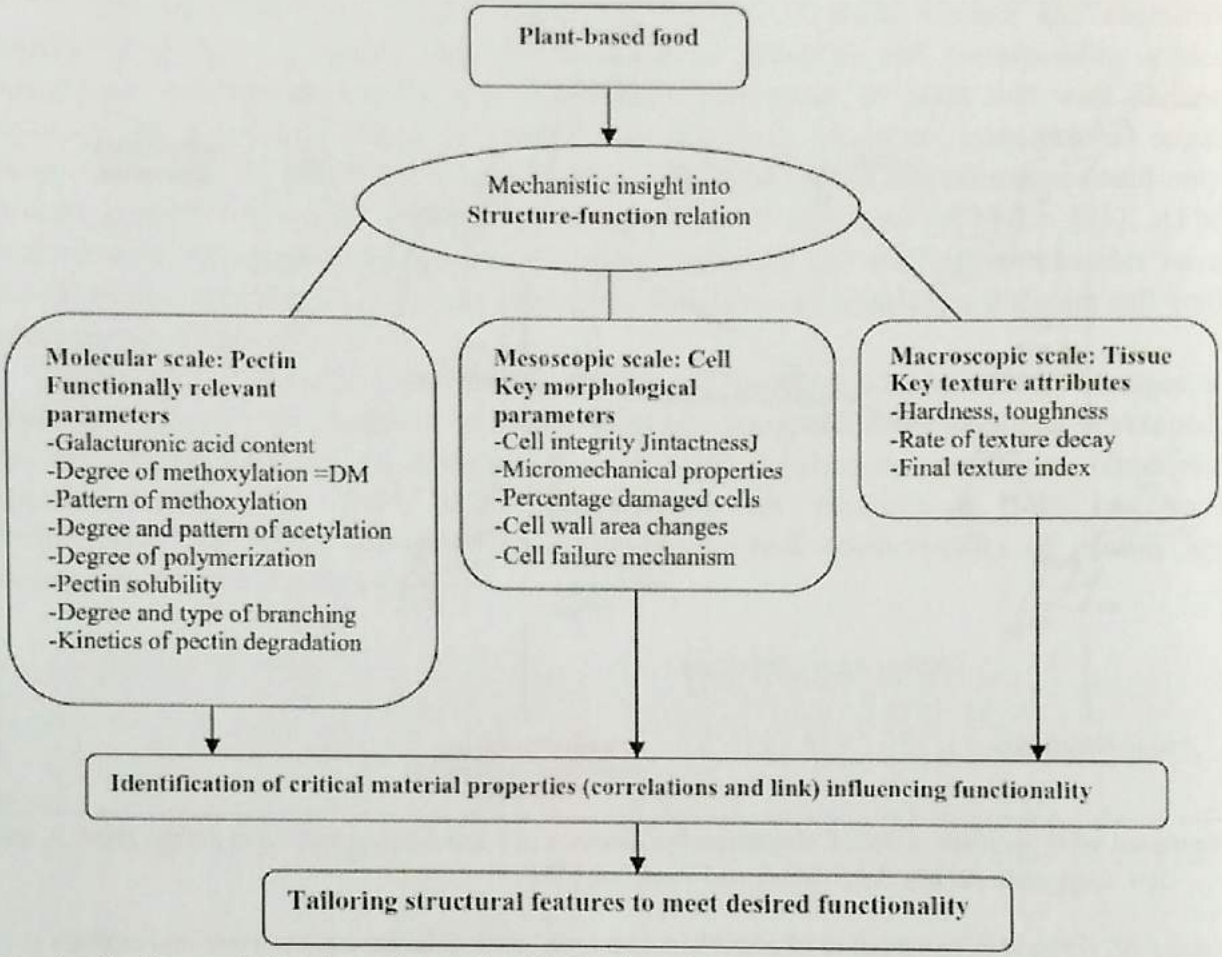

Reprinted with permission from Comprehensive Reviews in Food Science and Food Safety 2009, 8, 86-104. Copyright (2009), John Wiley and Sons, Inc [55].

Figure 23. An integrated approach toward intelligent engineering of the mechanical properties of plant-based foods.

Firmness is one of the most important quality indexes for fruits, which influences the acceptability of consumers. AFM results indicated that firmness was different among different ripe stages and cultivars. To explain the firmness differences between soft and crisp fruit cultivars, Yang and others (2009) compared the nanostructures of three kinds of pectins including WSP, CSP, and SSP by AFM. The results showed that soft peaches had short SSP chains, while the WSP and CSP chains were not much different between the two cultivars [39].

The neutral sugar-rich pectins from the primary cell wall of peach flesh might be the main differences of pectins and firmness between the two cultivar peaches. For Chinese cherry, firmer cherry group (crisp fruit) contained more percent of wide and short SSP chains than soft fruit, and the unripe groups contained more percent of wide and long SSP chains than corresponding ripe groups [11]. Chen and others (2009) investigated the morphological structures of hemicellulose of two cultivar cherries (crisp and soft) [15]. The widths of hemicellulose were significantly larger in crisp cherries than in soft ones, which suggested the thickness of hemicellulose chains may be related to cherry texture. Zhang and others (2010) found peach fruit firmness was not only dependent on the nanostructure of SSP, though SSP content showed the highest correlation with firmness among the three kinds of pectins (WSP,

CSP and SSP). Thus, there must be many other chemical changes involved in this process [41]. Similar results were reported in tomato CSP [53]. Compared with unripe groups, large CSP polymers were found degraded more with lower firmness in ripe tomatoes, which suggested the wide CSP chains decreased during ripening. Overall, morphology of CSP was closely related with firmness in different cultivars and ripening stages.

3.3. Effects of Postharvest Treatment on Pectin Morphology and Physicochemical Changes

The combination of AFM technique with physicochemical analysis was useful in revealing the fundamentals of postharvest fruit softening and finding solutions to extend fruit shelf life. Effects of controlled atmosphere storage on nanostructural information of WSP, CSP and SSP of peaches examined by AFM were reported [33, 37, 38]. The aggregates of these three kinds of pectins separated gradually with storage time. Meantime, frequency of chains with small length and width value increased, suggesting that polysaccharides degraded along linear backbones as well as in side chains. The probability of small-width chains of peach pectins was more in the normal atmosphere group than that in controlled atmosphere storage group, which was consistent with that degradation of pectin chains was slower in controlled atmosphere storage than normal atmosphere storage.

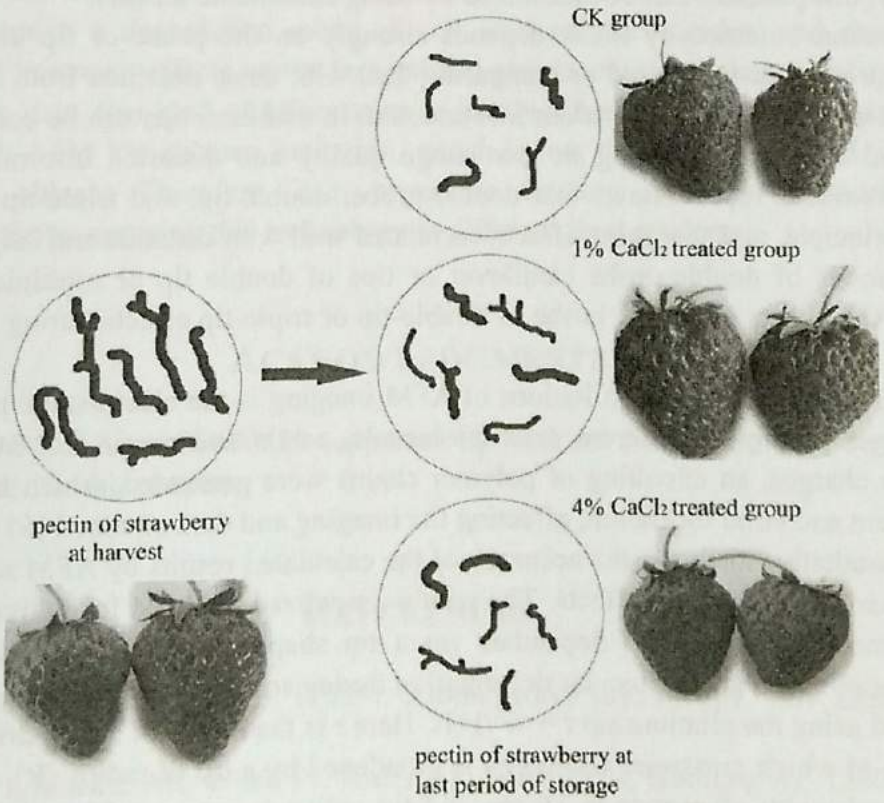

Reprinted from Food Chemistry 2011, 126, Chen F, et al., Quality attributes and cell wall properties of strawberries (*Fragaria annanassa Duch.*) under calcium chloride treatment, 458, Copyright (2011), with permission from Elsevier [59].

Figure 24. Schematic image of strawberry pectin degradation after $CaCl_2$ treatment during cold storage.

Liu and others (2009) reported the effects of calcium treatment on physicochemical properties and nanostructures of CSP of apricot during cold storage [40]. Apricot firmness did not change with the contents but its changes were consistent with the morphology changes of CSP. The branching structures of CSP decreased, meanwhile, the frequencies of CSP chains with small widths and lengths increased during storage. The side chains of CSP degraded during storage possibly due to the action of pectin-degrading enzymes, which destroyed the carboxyl-based crosslinking sites. Calcium treatment, moreover, delayed the changes of physicochemical properties and the degradation of CSP by strengthening the ionic crosslinkages among pectin molecules. All these results provided us with useful information to investigate the quality indexes from structural studies at nanoscale. Figure 24 shows schematic images of strawberry pectin degradation after $CaCl_2$ treatment during cold storage, which was obtained by combining results from AFM morphology and physicochemical analysis [59].

4. Limitations of AFM and Perspectives

Unfortunately, there are some limitations existed in AFM molecular imaging. The main problem is caused by crystallization of buffers and distortion of deposited samples. Fortunately, this problem can be minimized by using sublimable buffers.

Information obtained by AFM depends strongly on the probe or tip used. Therefore, when interpreting data acquired or comparing data with those obtained from other analyses, probe and tip effects have to be taken into account. In addition, tips can be contaminated due to soft food materials, resulting in low image quality and distorted information from the scanning. Previous report shows that double-probe, double-tip, and triple-tip effects shared the same principle, and that these effects correlated well with distance and height differences between probes of double-probe cantilever or tips of double tip or multiple-tip probes. It reminded AFM users of double probe or double-tip or triple-tip effects during AFM scanning [60].

A third awareness of the limitations of AFM imaging is the electrostatic repulsion of the same charges present in different macromolecuels, pectin and mucin, for instance. Due to these same charges, an uncoiling of polymer chains were generated, which facilitated chain entanglement and bond formation, affecting the imaging and data obtained [61].

For quantitative analysis, the accuracy of the calculated results by AFM software may be compromised by broadening effects. The widths visualized by AFM for individual molecules are broadened by an amount dependant upon tip shape and size, and additional factors including scan speed and molecular deformation during scanning. The pure geometrical effect is estimated using the relationship $r = w^2/16R$. Here r is the radius of a cylindrical molecule of the sample of which measured width (w) is broadened by a tip of radius (R). For instance, if the measured width of pectins is 15 nm and tip radius is between 20 and 40 nm, then the radius of molecular rods will be between 0.35 and 0.7 nm [16].

Currently, many traditional methods applied to characterize the quality of postharvest fruits have their strengths, weaknesses, and special applications. However, AFM is advantageous, being promising and useful in elucidating the fundamental changes of fruit

physicochemical changes and investigating the effects of numerous processing technologies on extending the shelf life of fruits, although many food macromolecules may have weak abilities of attaching to mica or other support surfaces. It is essential to develop methods for modifying the support surface or adding other chemicals to allow the macromolecules to attach to the surface well.

The nanostructural changes of fruit cell wall polysaccharides obtained by AFM are crucial reflecting the cell wall degradation during fruit texture softening. Serials of reports have confirmed that the morphological structures of cell wall polysaccharides had close relationship with fruit physicochemical properties. AFM may be an effective method to elucidate the degradation of polysaccharides.

CONCLUSION

AFM has been applied to characterize delicate molecular structures and molecular interactions. It has successfully provided qualitative and quantitative information of food macromolecule structures and molecular interactions, with or without molecular manipulation. AFM can provide new knowledge that relates to food processing, handling and storage, thus the results from AFM scanning help guide food processing and storage.

AFM results modified our previous understanding of pectin molecular structures, furthered the knowledge about the fundamentals of textural changes of fruits during postharvest through a degradation mode of cell wall polysaccharides, and elucidated the processing and treatment effects on the textural and physicochemical changes of fruits during postharvest. To date, this kind of information is hardly achieved by other techniques except AFM, although AFM has its own limitation, which is that there is no standard protocol for various study objects. Therefore, it is urgent to develop standard methodologies and procedures for better applying this technology in different food products.

ACKNOWLEDGMENTS

Projects 31071617 and 30600420 supported by National Natural Science Foundation of China contributed to this chapter.

REFERENCES

[1] Blanchard CR, Campbell JB. (1995). Atomic-force microscopy. *Adv Mater Process* 148, 62.

[2] Morris VJ, Mackie AR, Wilde PJ, Kirby AR, Mills ECN, Gunning AP. (2001). Atomic force microscopy as a tool for interpreting the rheology of food biopolymers at the molecular level. *Lebensm-Wiss Technol* 34, 3-10.

[3] Yang H, Wang Y, Lai S, An H, Li Y, Chen F. (2007). Application of atomic force microscopy as a nanotechnology tool in food science. *J Food Sci* 72, R65-75.

[4] Wilson RA, Bullen HA. (2007). Ched 643-preparation of polyether substituted poly(phenylenevinylenes) for use in light emitting devices. *Abstr Pap Am Chem* S 233, 96-.

[5] Yang HS, Wang YF, Lai SJ, An HJ, Li YF, Chen FS. (2007). Application of atomic force microscopy as a nanotechnology tool in food science. *J Food Sci* 72, R65-R75.

[6] Morris VJ, Kirby AR, Gunning AP. (1999). Using atomic force microscopy to probe food biopolymer functionality. *Scanning* 21, 287-92.

[7] Yang HS, An HJ, Li YF. (2006). Manipulate and stretch single pectin molecules with modified molecular combing and fluid fixation techniques. *Eur Food Res Technol* 223, 78-82.

[8] Kirby AR, MacDougall AJ, Morris VJ. (2008). Atomic force microscopy of tomato and sugar beet pectin molecules. *Carbohyd Polym* 71, 640-7.

[9] Sriamornsak P, Thirawong N, Nunthanid J, Puttipipatkhachorn S, Thongborisute J, Takeuchi H. (2008). Atomic force microscopy imaging of novel self-assembling pectin-liposome nanocomplexes. *Carbohyd Polym* 71, 324-9.

[10] Morris VJ, Gromer A, Kirby AR, Bongaerts RJM, Gunning AP. (2011). Using afm and force spectroscopy to determine pectin structure and (bio) functionality. *Food Hydrocolloid* 25, 230-7.

[11] Zhang LF, Chen FS, An HJ, Yang HS, Sun XY, Guo XF, et al. (2008). Physicochemical properties, firmness, and nanostructures of sodium carbonate-soluble pectin of 2 chinese cherry cultivars at 2 ripening stages. *J Food Sci* 73, N17-N22.

[12] Fantner GE, Schitter G, Kindt JH, Ivanov T, Ivanova K, Patel R, et al. (2006). Components for high speed atomic force microscopy. *Ultramicroscopy* 106, 881-7.

[13] Adams EL, Kroon PA, Williamson G, Morris VJ. (2003). Characterisation of heterogeneous arabinoxylans by direct imaging of individual molecules by atomic force microscopy. *Carbohyd Res* 338, 771-80.

[14] Watabe H, Nakajima K, Sakai Y, Nishi T. (2006). Dynamic force spectroscopy on a single polymer chain. *Macromolecules* 39, 5921-5.

[15] Chen FS, Zhang LF, An HJ, Yang HS, Sun XY, Liu H, et al. (2009). The nanostructure of hemicellulose of crisp and soft chinese cherry (prunus pseudocerasus l.) cultivars at different stages of ripeness. *Lwt-Food Sci Technol* 42, 125-30.

[16] Morris VJ, Gunning AP, Kirby AR, Round A, Waldron K, Ng A. (1997). Atomic force microscopy of plant cell walls, plant cell wall polysaccharides and gels. *Int J Biol Macromol* 21, 61-6.

[17] Ding SY, Himmel ME. (2006). The maize primary cell wall microfibril: A new model derived from direct visualization. *J Agr Food Chem* 54, 597-606.

[18] Adams EL, Kroon PA, Williamson G, Morris VJ. (2005). Afm studies of water-soluble wheat arabinoxylans - effects of esterase treatment. *Carbohyd Res* 340, 1841-5.

[19] Gunning AP, Mackie AR, Kirby AR, Kroon P, Williamson G, Morris VJ. (2000). Motion of a cell wall polysaccharide observed by atomic force microscopy. *Macromolecules* 33, 5680-5.

[20] Morris T, Sun J, Szulczewski G. (2003). Measurement of the chemical and morphological changes that occur on gold surfaces following thermal desorption and acid dissolution of adsorbed mercury. *Anal Chim Acta* 496, 279-87.

[21] Round AN, Rigby NM, MacDougall AJ, Ring SG, Morris VJ. (2001). Investigating the nature of branching in pectin by atomic force microscopy and carbohydrate analysis. *Carbohyd Res* 331, 337-42.

[22] Ridout MJ, Brownsey GJ, Gunning AP, Morris VJ. (1998). Characterisation of the polysaccharide produced by acetobacter xylinum strain cr1/4 by light scattering and atomic force microscopy. *Int J Biol Macromol* 23, 287-93.

[23] Gunning AP, Kirby AR, Ridout MJ, Brownsey GJ, Morris VJ. (1996). Investigation of gellan networks and gels by atomic force microscopy. *Macromolecules* 29, 6791-6.

[24] Gunning AP, Giardina TP, Faulds CB, Juge N, Ring SG, Williamson G, et al. (2003). Surfactant-mediated solubilisation of amylose and visualisation by atomic force microscopy. *Carbohyd Polym* 51, 177-82.

[25] Ovodova RG, Popov SV, Bushneva OA, Golovchenko VV, Chizhov AO, Klinov DV, et al. (2006). Branching of the galacturonan backbone of comaruman, a pectin from the marsh cinquefoil comarum palustre l. *Biochemistry-Moscow+* 71, 538-42.

[26] Round AN, MacDougall AJ, Ring SG, Morris VJ. (1997). Unexpected branching in pectin observed by atomic force microscopy. *Carbohyd Res* 303, 251-3.

[27] Adams EL, Kroon PA, Williamson G, Gilbert HJ, Morris VJ. (2004). Inactivated enzymes as probes of the structure of arabinoxylans as observed by atomic force microscopy. *Carbohyd Res* 339, 579-90.

[28] Morris VJ, Gunning AP, Faulds CB, Williamson G, Svensson B. (2005). Afm images of complexes between amylose and aspergillus niger glucoamylase mutants, native, and mutant starch binding domains: A model for the action of glucoamylase. *Starch-Starke* 57, 1-7.

[29] Decho AW. (1999). Imaging an alginate polymer gel matrix using atomic force microscopy. *Carbohyd Res* 315, 330-3.

[30] Gunning AP, Cairns P, Kirby AR, Round AN, Bixler HJ, Morris VJ. (1998). Characterising semi-refined iota-carrageenan networks by atomic force microscopy. *Carbohyd Polym* 36, 67-72.

[31] Vardhanabhuti B, Ikeda S. (2006). Isolation and characterization of hydrocolloids from monoi (cissampelos pareira) leaves. *Food Hydrocolloid* 20, 885-91.

[32] Gunning AP, Morris VJ, AlAssaf S, Phillips GO. (1996). Atomic force microscopic studies of hylan and hyaluronan. *Carbohyd Polym* 30, 1-8.

[33] Yang HS, Feng GP, An HJ, Li YF. (2006). Microstructure changes of sodium carbonate-soluble pectin of peach by afm during controlled atmosphere storage. *Food Chem* 94, 179-92.

[34] Sriamornsak P, Wattanakorn N, Nunthanid J, Puttipipatkhachorn S. (2008). Mucoadhesion of pectin as evidence by wettability and chain interpenetration. *Carbohyd Polym* 74, 458-67.

[35] Li B, Xie BJ. (2006). Single molecular chain geometry of konjac glucomannan as a high quality dietary fiber in east asia. *Food Res Int* 39, 127-32.

[36] Ikeda S, Nitta Y, Kim BS, Temsiripong T, Pongsawatmanit R, Nishinari K. (2004). Single-phase mixed gels of xyloglucan and gellan. *Food Hydrocolloid* 18, 669-75.

[37] Yang HS, An HJ, Feng GP, Li YF, Lai SJ. (2005). Atomic force microscopy of the water-soluble pectin of peaches during storage. *Eur Food Res Technol* 220, 587-91.

[38] Yang HS, Lai SJ, An HJ, Li YF. (2006). Atomic force microscopy study of the ultrastructural changes of chelate-soluble pectin in peaches under controlled atmosphere storage. *Postharvest Biol Tec* 39, 75-83.

[39] Yang HS, Chen FS, An HJ, Lai SJ. (2009). Comparative studies on nanostructures of three kinds of pectins in two peach cultivars using atomic force microscopy. *Postharvest Biol Tec* 51, 391-8.

[40] Liu H, Chen FS, Yang HS, Yao YZ, Gong XZ, Xin Y, et al. (2009). Effect of calcium treatment on nanostructure of chelate-soluble pectin and physicochemical and textural properties of apricot fruits. *Food Res Int* 42, 1131-40.

[41] Zhang LF, Chen FS, Yang HS, Sun XY, Liu H, Gong XZ, et al. (2010). Changes in firmness, pectin content and nanostructure of two crisp peach cultivars after storage. *Lwt-Food Sci Technol* 43, 26-32.

[42] Kirby AR, Ng A, Waldron KW, Morris VJ. (2006). Afm investigations of cellulose fibers in bintje potato (solanum tuberosum l.) cell wall fragments. *Food Biophys* 1, 163-7.

[43] Hansma HG, Kim KJ, Laney DE, Garcia RA, Argaman M, Allen MJ, et al. (1997). Properties of biomolecules measured from atomic force microscope images: A review. *J Struct Biol* 119, 99-108.

[44] Hershko V, Nussinovitch A. (1998). Physical properties of alginate-coated onion (allium cepa) skin. *Food Hydrocolloid* 12, 195-202.

[45] Hershko V, Weisman D, Nussinovitch A. (1998). Method for studying surface topography and roughness of onion and garlic skins for coating purposes. *J Food Sci* 63, 317-21.

[46] Yang HS, An HJ, Feng GP, Li YF. (2005). Visualization and quantitative roughness analysis of peach skin by atomic force microscopy under storage. *Lwt-Food Sci Technol* 38, 571-7.

[47] Custance O, Perez R, Morita S. (2009). Atomic force microscopy as a tool for atom manipulation. *Nat Nanotechnol* 4, 803-10.

[48] Carpita NC, Gibeaut DM. (1993). Structural models of primary-cell walls in flowering plants - consistency of molecular-structure with the physical-properties of the walls during growth. *Plant* J 3, 1-30.

[49] Himmel ME, Ding SY, Johnson DK, Adney WS, Nimlos MR, Brady JW, et al. (2007). Biomass recalcitrance: Engineering plants and enzymes for biofuels production. *Science* 315, 804-7.

[50] Nishiyama Y, Langan P, Chanzy H. (2002). Crystal structure and hydrogen-bonding system in cellulose ibeta from synchrotron x-ray and neutron fiber diffraction. *J Am Chem Soc* 124, 9074-82.

[51] Perez S, Rodriguez-Carvajal MA, Doco T. (2003). A complex plant cell wall polysaccharide: Rhamnogalacturonan ii. A structure in quest of a function. Biochimie 85, 109-21.

[52] Abied H, Brulet A, Guenet JM. (1990). Physical gels from pvc - molecular-structure of pregels and gels by low-angle neutron-scattering. *Colloid Polym Sci* 268, 403-13.

[53] Xin Y, Chen FS, Yang HS, Zhang PL, Deng Y, Yang B. (2010). Morphology, profile and role of chelate-soluble pectin on tomato properties during ripening. *Food Chem* 121, 372-80.

[54] Lesniewska E, Adrian M, Klinguer A, Pugin A. (2004). Cell wall modification in grapevine cells in response to uv stress investigated by atomic force microscopy. *Ultramicroscopy* 100, 171-8.

[55] Van Buggenhout S, Sila DN, Duvetter T, Van Loey A, Hendrickx M. (2009). Pectins in processed fruits and vegetables: Part iii - texture engineering. *Compr Rev Food Sci* F 8, 105-17.

[56] Zhang L, Chen F, An H, Yang H, Sun X, Guo X, et al. (2008). Physicochemical properties, firmness, and nanostructures of sodium carbonate-soluble pectin of 2 chinese cherry cultivars at 2 ripening stages. *J Food Sci* 73, N17-22.

[57] Ralet MC, Dronnet V, Buchholt HC, Thibault JF. (2001). Enzymatically and chemically de-esterified lime pectins: Characterisation, polyelectrolyte behaviour and calcium binding properties. *Carbohyd Res* 336, 117-25.

[58] Kirby AR, MacDougall AJ, Morris VJ. (2006). Sugar beet pectin-protein complexes. *Food Biophys* 1, 51-6.

[59] Chen FS, Liu H, Yang HS, Lai SJ, Cheng XL, Xin Y, et al. (2011). Quality attributes and cell wall properties of strawberries (fragaria annanassa duch.) under calcium chloride treatment. *Food Chem* 126, 450-9.

[60] Chen Y, Cai J, Liu M, Zeng G, Feng Q, Chen Z. (2004). Research on double-probe, double- and triple-tip effects during atomic force microscopy scanning. *Scanning* 26, 155-61.

[61] Sriamornsak P, Wattanakorn N, Takeuchi H. (2010). Study on the mucoadhesion mechanism of pectin by atomic force microscopy and mucin-particle method. *Carbohyd Polym* 79, 54-9.